[25] Y.I. Sheline, P.W. Wang, M.H. Gado, J.G. Csernansky, M.W. Vannier, Hippocampal atrophy in recurrent major depression, Proc. Natl. Acad. Sci. U. S. A. 93 (1996) 3908–3913.
[26] A.C. Silva, C. Stevens, S. Tonegawa, Y. Wang, Deficient hippocampal long-term potentination in α-calcium-calmodulin kinase II mutant mice, Science 257 (1992) 201–206.
[27] J.D. Sweatt, The neuronal MAP kinase cascade: a biochemical signal integration system subserving synaptic plasticity and memory, J. Neurochem. 76 (2001) 1–10.
[28] J. Takeda, H. Yano, S. Eng, G.I. Bell, A molecular inventory of human pancreatic islets: sequence analysis of 1000 cDNA clones, Hum. Mol. Genet. 2 (1993) 1793–1798.
[29] H. van Praag, G. Kempermann, F.H. Gage, E. Gould, P. Tanapat, Running increase cell prolification and neurogenesis in the adult mouse dentate gyrus, Nat. Neurosci. 2 (1999) 266–270.
[30] E.A. Young, R.F. Haskett, V. Murphy-Weinberg, S.J. Watson, H. Akil, Loss of glucocorticoid fast feedback in depression, Arch. Gen. Psychiatry 48 (1991) 693–699.

Available online at www.sciencedirect.com
SCIENCE DIRECT
Biochemical and Biophysical Research Communications 321 (2004) 510–513
BBRC
www.elsevier.com/locate/ybbrc

Acute effect of corticosterone on *N*-methyl-D-aspartate receptor-mediated Ca^{2+} elevation in mouse hippocampal slices

Satoru Sato [a], Hiromi Osanai [a], Toshihiro Monma [a], Tokiko Harada [a], Ayumi Hirano [a], Minoru Saito [a,*], Suguru Kawato [b]

[a] *Department of Physics and Applied Physics, College of Humanities and Sciences, Nihon University, 3-25-40 Sakurajosui, Setagaya-ku, Tokyo 156-8550, Japan*
[b] *Department of Biophysics and Life Sciences, Graduate School of Arts and Sciences, University of Tokyo at Komaba, Tokyo 153-8902, Japan*

Received 10 June 2004

Abstract

We examined the rapid effects of corticosterone (CORT) on *N*-methyl-D-aspartate (NMDA) receptor-mediated Ca^{2+} signals in adult mouse hippocampal slices by using Ca^{2+} imaging technique. Application of NMDA caused a transient elevation of intracellular Ca^{2+} concentration followed by a decay to a plateau within 150 s. The 30 min preincubation of CORT induced a significant decrease of the peak amplitude of NMDA-induced Ca^{2+} elevation in the CA1 region. The rapid effect of CORT was induced at a stress-induced level (0.4–10 μM). Because the membrane non-permeable bovine serum albumin-conjugated CORT also induced a similar rapid effect, the rapid effect of CORT might be induced via putative surface CORT receptors. In contrast, CORT induced no significant effects on NMDA-induced Ca^{2+} elevation in the dentate gyrus. In the CA3 region, CORT effects were not evaluated, because the marked elevation of NMDA-induced Ca^{2+} signals was not observed there.

Keywords: Acute effect; Ca^{2+} signals; Corticosterone; Glucocorticoids; NMDA receptor; Hippocampus

Corticosterone (CORT) is a principal glucocorticoid synthesized in the rodent adrenal cortex and secreted in response to stress. There are a series of studies about the chronic and genomic effects of corticosteroids in the hippocampus [1,2]. The stress-induced increase in CORT secretion is known to produce neuronal cell damage. Exogenous application of a high dose of CORT has been shown to elicit the neuronal atrophy in the hippocampus [3]. Rats exposed to restraint stress for three weeks exhibited neuronal atrophy identical to that seen in rats treated with a high dose of CORT for three weeks [4]. In addition to these classical genomic effects, which are actuated via intracellular steroid receptors, glucocorticoids act acutely on neuronal excitability [5,6]. The long-term potentiation (LTP) of the population spike amplitude was also acutely (within 1 h) suppressed by a high concentration of glucocorticoids [7]. It has also been demonstrated that CORT dosage for 20 min significantly suppresses the development of LTP in the CA1 region of 4-week-old rat hippocampal slices [8,9].

It is well known that Ca^{2+} influx via *N*-methyl-D-aspartate (NMDA) receptors plays a crucial role in the induction of LTP. The rapid effects of CORT (appearing within 30 min) on NMDA-induced Ca^{2+} signal transduction, however, have not been well elucidated in the hippocampus. In the present study, we examined the rapid effects of CORT on NMDA receptor-mediated Ca^{2+} signals in mouse hippocampal slices by using Ca^{2+} imaging technique. An advantage of mouse hippocampal slices was that we could measure the CA1, CA3, and dentate gyrus regions simultaneously because the whole hippocampus fell within the microscope field. As a

* Corresponding author. Fax: +81-3-5317-9432.
E-mail address: msaito@chs.nihon-u.ac.jp (M. Saito).

0006-291X/$ - see front matter © 2004 Elsevier Inc. All rights reserved.
doi:10.1016/j.bbrc.2004.06.168

result, the 30 min preincubation of CORT induced a significant decrease of the peak amplitude of NMDA-induced Ca^{2+} elevation in the CA1 region. The rapid effect of CORT region was induced at a stress-induced level (0.4–10 μM). In contrast, CORT induced no significant effects on NMDA-induced Ca^{2+} elevation in the dentate gyrus. In the CA3 region, CORT effects were not evaluated, because the marked elevation of NMDA-induced Ca^{2+} signals was not observed there.

Materials and methods

Brain slices (coronal, 300 μm thick) were prepared from 7-week-old male ddY mice after exposure to an overdose of diethyl ether anesthesia. In order to stabilize the plasma glucocorticoid level, mice used in all experiments were decapitated at the same moment (10 a.m.) in the circadian cycle. Following decapitation, the brain was quickly removed and placed in ice-cold oxygenated artificial cerebrospinal fluid (ACSF) (composition in mM: NaCl 124, KCl 5, $CaCl_2$ 2, $NaHCO_3$ 22, $MgSO_4$ 2, NaH_2PO_4 1.24, glucose 10, pH 7.4, and bubbled with 95% O_2/5% CO_2). Slices were then prepared using a microslicer (DTK-1000; Dosaka-EM, Kyoto, Japan). The slices were recovered in ACSF at 30 °C for 60 min and held at room temperature until use. All experiments using animals were conducted in accordance with the institutional guidelines.

Measurement of intracellular Ca^{2+} concentration $[Ca^{2+}]_i$ was performed using the Ca^{2+}-sensitive indicator fura-2. Prior to Ca^{2+} signal measurements, the slices were loaded for 30 min at room temperature with 10 μM fura-2/AM [from 1 mM stock solution in dimethyl sulfoxide (DMSO)] in the presence of 0.01% cremophore EL in 7.2 mL ACSF. After loading with fura-2, the slices were washed in ACSF for 30 min and then preincubated with CORT or bovine serum albumin-conjugated CORT (BSA–CORT) solution for 30 min. CORT and BSA–CORT solutions were prepared at the appropriate dilution with low Mg^{2+} ACSF (control solution) (composition in mM: NaCl 124, KCl 5, $CaCl_2$ 2, $NaHCO_3$ 22, $MgSO_4$ 0.1, NaH_2PO_4 1.24, glucose 10, pH 7.4, and gassed with 5% CO_2/95% O_2) from the stock solution in DMSO. The final concentration of DMSO was less than 0.05% in each case.

For fluorescence measurements of $[Ca^{2+}]_i$, a digital fluorescence microscope system, consisting of an inverted microscope (TE 300; Nikon, Tokyo, Japan) equipped with a xenon lamp for excitation and a CCD camera (C4742-95; Hamamatsu Photonics, Hamamatsu, Japan), was used. Preincubated brain slices were placed in a chamber on the microscope stage. The whole hippocampus fell within the microscope field by using a 4× fluorescence objective (Nikon, Tokyo, Japan). The slices were then perfused with the CORT or BSA–CORT solution kept at 30 °C. At 150 s after the onset of recording the perfusing solution was replaced by the solution containing 1 mM NMDA.

For fura-2 measurements, the excitation wavelength varied discretely between 340 and 380 nm, and $[Ca^{2+}]_i$ was expressed as F340/F380, which is the ratio of the 510 nm fluorescence intensity at 340 nm excitation (F340) to that at 380 nm excitation (F380). In each acquisition trial, consecutive fluorescence images were acquired at 5 s intervals for 350 s. Fig. 1 shows examples of a series of obtained images. The fluorescence images were then analyzed with AQUACOSMOS system (Ver.1.3; Hamamatsu Photonics, Hamamatsu, Japan). Twelve ROIs (regions of interest: 5 × 5 pixels) were put on the cell body layer of each hippocampal subfield, and the fluorescence data of those ROIs were averaged.

The data were expressed as means ± SEM. Student's t test was utilized to test the significance of observed differences between groups. Significance was set at $p < 0.005$.

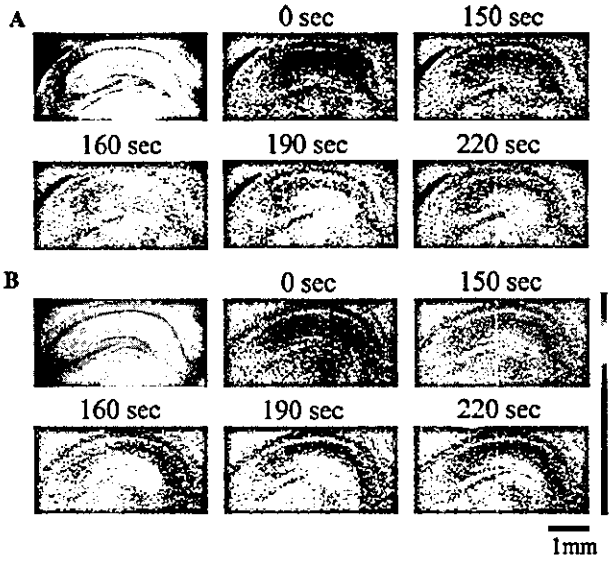

Fig. 1. Fluorescence images of mouse hippocampal slices (A) without the CORT dosage and (B) with the 1 μM CORT dosage. Upper left one of each column is a fluorescence image of a fura-2-loaded slice excited at 380 nm. The other pseudo-colored images demonstrate $[Ca^{2+}]_i$ in the slice. The color bar shows the ratio of the fluorescence intensity of fura-2 excited at 340 and 380 nm, which expresses $[Ca^{2+}]_i$, from blue (low $[Ca^{2+}]_i$) to red (high $[Ca^{2+}]_i$). The time above each pseudo-colored image shows the time from the onset of experiment. At 150 s after the onset of experiment, 1 mM NMDA was applied.

Results

Fig. 2 shows the typical time courses of NMDA-induced Ca^{2+} signal obtained from (A) the CA1 region and (B) the dentate gyrus. The response to continuous NMDA exposure was characterized by a transient elevation in $[Ca^{2+}]_i$ followed by a decay to a plateau within 150 s (see also Fig. 1). The transient elevation in $[Ca^{2+}]_i$ was due to NMDA receptor-mediated Ca^{2+} influx, because no response to NMDA application was observed in the slices preincubated with 100 μM of NMDA antagonist MK-801 (Fig. 2). In the control condition without CORT or BSA–CORT preincubation, the peak amplitudes of $[Ca^{2+}]_i$ elevation, calculated as an increase (Δ(F340/F380)) in F340/F380 from baseline level, were 0.40 ± 0.03 ($n = 7$) in the CA1 region, 0.05 ± 0.01 ($n = 7$) in the CA3 region, and 0.22 ± 0.01 ($n = 7$) in the dentate gyrus. These average values were set to 100%. In the CA1 region, the peak amplitude of $[Ca^{2+}]_i$ elevation was decreased by preincubation with CORT in a dose-dependent manner. The decreased peak amplitudes were $49.4 \pm 9.9\%$ ($n = 5$, $p < 0.005$), $43.0 \pm 7.7\%$ ($n = 9$), and $30.4 \pm 2.0\%$ ($n = 5$) at 0.4, 1, and 10 μM of CORT compared with control (Fig. 3A). In addition, preincubation with 1 μM BSA–CORT (approximately 20 CORT molecules per BSA molecule) also induced a decrease in the peak amplitude ($30.2 \pm 5.0\%$, $n = 5$, $p <$ 0.005). In contrast,

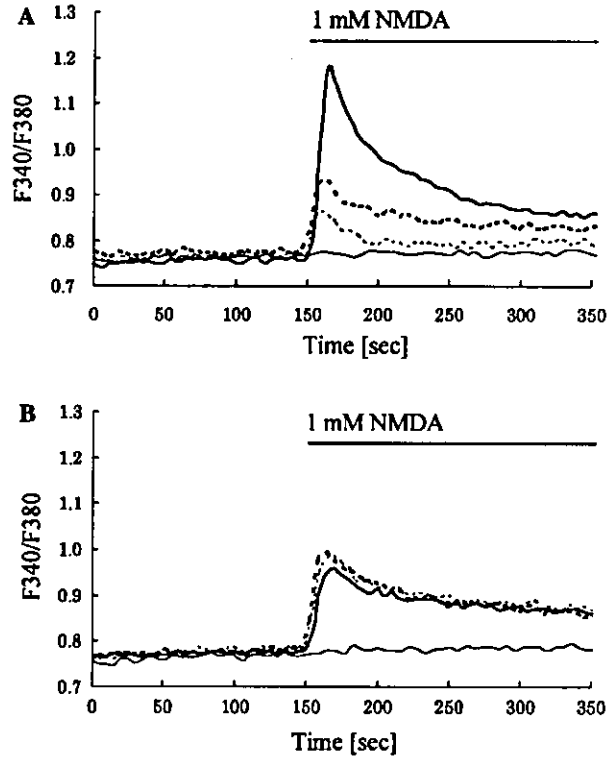

Fig. 2. Typical time courses of NMDA-induced Ca^{2+} signal in (A) the CA1 region and (B) the dentate gyrus. The vertical scale (F340/F380) is the ratio of the fluorescence intensity of fura-2 excited at 340 and 380 nm. Without the CORT dosage, 1 mM NMDA application induced a transient elevation in $[Ca^{2+}]_i$ followed by a decay to a plateau (control: thick line). The Ca^{2+} signal almost disappeared with the 100 μM MK-801 dosage (thin line). With the dosage of CORT, the $[Ca^{2+}]_i$ elevation was decreased compared with control in the CA1 region (1 μM CORT, thick-dotted line; 10 μM CORT, thin-dotted line). In contrast, the CORT dosage induced no significant effect on the Ca^{2+} signal in the dentate gyrus.

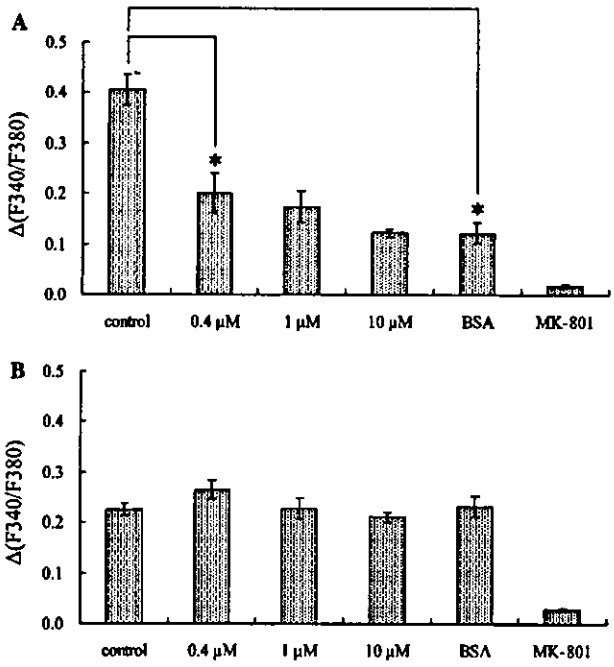

Fig. 3. The effect of CORT on the peak amplitude of NMDA-induced Ca^{2+} signal elevation in (A) the CA1 region and (B) the dentate gyrus. The vertical scale (Δ(F340/F380)) is the peak amplitude of F340/F380 from baseline. The concentrations below the figures show the dosed concentrations of CORT. BSA and MK-801 show the dosage of 1 μM BSA–CORT and 100 μM MK-801, respectively. The data are expressed as means ± SEM. The $[Ca^{2+}]_i$ elevation was significantly suppressed at 0.4 μM CORT and 1 μM BSA–CORT in the CA1 region. $^*p < 0.005$ compared from control value.

preincubation with neither CORT nor BSA–CORT significantly changed the peak amplitude of $[Ca^{2+}]_i$ elevation in the dentate gyrus: the peak amplitudes were 117.8 ± 8.5% ($n = 5$), 101.1 ± 9.4% ($n = 9$), and 93.5 ± 4.6% ($n = 5$) at 0.4, 1, and 10 μM of CORT, and 103.2 ± 9.1% ($n = 5$) at 1 μM BSA–CORT compared with control (Fig. 3B). In the CA3 region, CORT and BSA–CORT effects were not evaluated, because the marked elevation of NMDA-induced Ca^{2+} signals was not observed there.

Discussion

In the present study, we examined the rapid effects of CORT on NMDA receptor-mediated Ca^{2+} signals in adult mouse hippocampal slices by using Ca^{2+} imaging technique. An advantage of mouse hippocampal slices was that we could measure the CA1, CA3, and dentate gyrus regions simultaneously because the whole hippocampus fell within the microscope field. Concerning rat hippocampal slices, we need to use different slices in order to compare the CA1, CA3, and dentate gyrus regions, resulting in losing accuracy of the relative levels for the $[Ca^{2+}]_i$ elevation. In addition, the heterogeneous effect of CORT between the CA1, CA3, and dentate gyrus regions could not be examined in our previous study using cultured neonatal hippocampal neurons [10], because all the neurons were mixed up there.

The present results showed the rapid effects (within 30 min) on NMDA-induced Ca^{2+} signals particularly in the CA1 region. The transient elevation in $[Ca^{2+}]_i$ induced by NMDA application was significantly suppressed to 49.4% at 0.4 μM CORT in the CA1 region. The increases of CORT concentration to 1.0 and 10 μM gave only a small additional decrease to 43.0 and 30.4%. The CORT effect in the CA1 region is physiologically significant, because rats subjected to immobilization-stress for 1 h were reported to show approximately 2 μM CORT in blood plasma [11]. In our previous study, a similar suppressive effect of CORT was also found in the CA1 region of 4-week-old rat hippocampal slices, in which the peak amplitude of $[Ca^{2+}]_i$ elevation decreased to 79.5% compared with control in the presence of 10 μM CORT (unpublished results).

On the other hand, CORT induced no significant effects on NMDA-induced Ca^{2+} elevation in the dentate gyrus as mentioned above. In the CA3 region, the marked elevation of NMDA-induced Ca^{2+} signals was not observed, although NMDA receptor should also be in the CA3 region. This reason is not clear at this stage.

The rapid effect of CORT on NMDA receptor-mediated Ca^{2+} signals was also found in the cultured neonatal hippocampal neurons in our previous study [10]. It should be noted that in the cultured neonatal hippocampal neurons, CORT induced the extreme prolongation of time duration of NMDA-induced Ca^{2+} elevation. However, the differences in the rapid effect of CORT between the previous study (using dissociated neonatal hippocampal neurons) and the present study (using adult mouse hippocampal slices) may not be controversial, because the age of hippocampal neurons was completely different between these preparations. Different effects of CORT may be due to the differences in molecular types of NMDA receptor subunits which are different between neonatal neurons (containing mainly NR2B) and adult neurons (containing both NR2A and NR2B) [12].

According to the classical view of the steroid action, CORT is thought to penetrate into the cytoplasm of neurons, bind to intracellular receptors, and induce genomic effects through new protein synthesis, resulting in the modulation of Ca^{2+} signals [1–4]. The present results suggested that CORT may bind to putative surface CORT receptors, because the membrane non-permeable BSA–CORT also induced a similar rapid effect. The possibility of genomic mechanisms can be also excluded as an explanation for the present CORT effect, because cycloheximide, an inhibitor of protein synthesis, did not abolish the effect of CORT on NMDA-induced Ca^{2+} signals.

A possible candidate for surface CORT receptors is a classical intracellular glucocorticoid receptor (e.g., GR, a type-2 receptor), which may be bound to plasma membranes. This idea is supported by reports that the immunoreactivity of antibodies against GR was associated with plasma membranes from hippocampal and hypothalamic neurons [13] and that specific CORT binding to neuronal membranes occurred in different brain areas with moderate affinity (K_d = 120 nM) [14,15]. Classical GRs are expressed in the cytoplasm of cultured hippocampal neurons [16]. GRs may drive both classical genomic pathways [17] and non-genomic pathways (the current study) in hippocampal neurons.

It is well known that Ca^{2+} influx via NMDA receptors plays a crucial role in the induction of LTP. The present results may have a good coincidence to the rapid suppressive effect of CORT found by electrophysiological investigations on the LTP in the CA1 region of 4-week-old rat hippocampal slices [8,9].

References

[1] S.M. Nair, T.R. Werkman, J. Craig, R. Finnell, M. Joels, J.H. Eberwine, Corticosteroid regulation of ion channel conductances and mRNA levels in individual hippocampal CA1 neurons, J. Neurosci. 18 (1998) 2685–2696.

[2] L.P. Reagan, B.S. McEwen, Contoversies surrounding glucocorticoid-mediated cell death in the hippocampus, J. Chem. Neuroanat. 13 (1997) 149–167.

[3] C.S. Wooly, E. Gould, B.S. McEwen, Exposure to excess glucocorticoids alters dendritic morphology of adult hippocampal pyramidal neurons, Brain Res. 531 (1990) 225–231.

[4] Y. Watanabe, E. Gould, B.S. McEwen, Stress induces atrophy of apical dendrites of hippocampal CA3 pyramidal neurons, Brain Res. 588 (1992) 341–345.

[5] P.W. Landfield, T.A. Pitler, Prolonged Ca^{2+} dependent after hyper-polarizations in hippocampal neurons of aged rats, Science 226 (1984) 1089–1092.

[6] S.J. Lupien, B.S. McEwen, The acute effect of corticosteroids on cognition: integration of animal and human model studies, Brain Res. Rev. 24 (1997) 1–27.

[7] C. Vidal, W. Jordan, W. Zieglgansberger, Corticosterone reduces the excitability of hippocampal pyramidal cells in vitro, Brain Res. 383 (1986) 54–59.

[8] S. Kawato, M. Yamada, T. Kimoto, Neurosteroids are 4th generation neuromessengers: cell biophysical analysis of steroid transduction, Adv. Biophys. 37 (2001) 1–30.

[9] K. Shibuya, N. Takata, Y. Hojo, A. Furukawa, N. Yasumasu, T. Kimoto, T. Enami, K. Suzuki, N. Tanabe, H. Ishii, H. Mukai, T. Takahashi, T. Hattori, S. Kawato, Hippocampal cytochrome P450s synthesize brain neurosteroids which are paracrine neuromodulators of synaptic signal transduction, Biochim. Biopys. Acta 1619 (2003) 301–316.

[10] T. Takahashi, T. Kimoto, N. Tanabe, T. Hattori, N. Yasumatsu, S. Kawato, Corticosterone acutely prolonged *N*-methyl-D-aspartate receptor-mediated Ca^{2+} elevation in cultured rat hippocampal neurons, J. Neurochem. 83 (2002) 1441–1451.

[11] S. Marinesco, C. Bonnet, R. Cespuglio, Influence of stress duration on the sleep rebound induced by immobilization in the rat: a possible role for corticosterone, Neuroscience 92 (1999) 921–933.

[12] H. Monyer, N. Burnashev, D.J. Laurie, B. Sakmann, P.H. Seeburg, Developmental and regional expression in the rat brain and functional properties of four NMDA receptors, Neuron 12 (1994) 529–540.

[13] Z. Lipositz, M.C. Bohn, Association of glucocorticoid receptor immunoreactivity with cell membrane and transport vesicles in hippocampal and hypothalamic neurons of the rat, J. Neurosci. Res. 35 (1993) 14–19.

[14] A.C. Towle, P.Y. Sze, Steroid binding to synaptic plasma membrane: differential binding of glucocorticoids and gonadal steroids, J. Steroid Biochem. 18 (1983) 135–143.

[15] Z. Guo, Y.Z. Chen, R.B. Xu, H. Fu, Binding characteristics of glucocorticoid receptor in synaptic plasma membrane from rat brain, Funct. Neurol. 10 (1995) 183–194.

[16] D.R. Packan, R.M. Sapolsky, Glucocorticoid endangerment of the hippocampus: tissue, steroid and receptor specificity, Neuroendocrinology 51 (1990) 613–618.

[17] M. Nishi, H. Ogawa, T. Ito, K.I. Matsuda, M. Kawata, Dynamic changes in subcellular localization of mineralocorticoid receptor in living cells: in comparison with glucocorticoid receptor using dual-color labeling with green fluorescent protein spectral variants, Mol. Endocrinol. 15 (2001) 1077–1092.

Adult male rat hippocampus synthesizes estradiol from pregnenolone by cytochromes P45017α and P450 aromatase localized in neurons

Yasushi Hojo*†, Taka-aki Hattori*†, Taihei Enami*, Aizo Furukawa†‡, Kumiko Suzuki*, Hiro-taka Ishii*, Hideo Mukai*†, John H. Morrison§, William G. M. Janssen§, Shiro Kominami¶, Nobuhiro Harada‖, Tetsuya Kimoto*†, and Suguru Kawato*†**

*Department of Biophysics and Life Sciences and †Core Research for Evolutional Science and Technology Project of Japan Science and Technology Corporation, Graduate School of Arts and Sciences, University of Tokyo at Komaba, Meguro, Tokyo 153, Japan; ‡Department of Psychiatry, Tokyo Metropolitan Matsuzawa Hospital, 2-1-1 Kamikitazawa, Setagaya, Tokyo 156, Japan; §Kastor Neurobiology of Aging Laboratories, Fishberg Research Center for Neurobiology, Mount Sinai School of Medicine, New York, NY 10029; ¶Faculty of Integrated Arts and Sciences, Hiroshima University, Higashi-hiroshima 739, Japan; and ‖Department of Biochemistry, School of Medicine, Fujita Health University, Toyoake, Aichi 470, Japan

Edited by Bruce S. McEwen, The Rockefeller University, New York, NY, and approved October 16, 2003 (received for review March 5, 2003)

In adult mammalian brain, occurrence of the synthesis of estradiol from endogenous cholesterol has been doubted because of the inability to detect dehydroepiandrosterone synthase, P45017α. In adult male rat hippocampal formation, significant localization was demonstrated for both cytochromes P45017α and P450 aromatase, in pyramidal neurons in the CA1–CA3 regions, as well as in the granule cells in the dentate gyrus, by means of immunohistochemical staining of slices. Only a weak immunoreaction of these P450s was observed in astrocytes and oligodendrocytes. ImmunoGold electron microscopy revealed that P45017α and P450 aromatase were localized in pre- and postsynaptic compartments as well as in the endoplasmic reticulum in principal neurons. The expression of these cytochromes was further verified by using Western blot analysis and RT-PCR. Stimulation of hippocampal neurons with *N*-methyl-D-aspartate induced a significant net production of estradiol. Analysis of radioactive metabolites demonstrated the conversion from [^{3}H]pregnenolone to [^{3}H]estradiol through dehydroepiandrosterone and testosterone. This activity was abolished by the application of specific inhibitors of cytochrome P450s. Interestingly, estradiol was not significantly converted to other steroid metabolites. Taken together with our previous finding of a P450scc-containing neuronal system for pregnenolone synthesis, these results imply that 17β-estradiol is synthesized by P45017α and P450 aromatase localized in hippocampal neurons from endogenous cholesterol. This synthesis may be regulated by a glutamate-mediated synaptic communication that evokes Ca^{2+} signals.

The hippocampal formation, essentially involved in learning and memory processes, is known to be a target for the neuromodulatory actions of hormones produced in the gonads. As both estradiol and testosterone may reach the brain via blood circulation, and extensive studies have been performed to investigate their role in modulating hippocampal plasticity and function (1–4). Evidence is emerging that estrogen exerts not only the chronic/genomic effects but also a rapid/nongenomic influence on hippocampal synaptic plasticity (2, 5). In addition to endocrine-derived hormones, recent experiments have demonstrated that hippocampal neurons may also be exposed to locally synthesized brain neurosteroids, such as pregnenolone (PREG) and its sulfated ester (6–9). Dehydroepiandrosterone (DHEA) has been found in the mammalian brain at concentrations greater than that in plasma (6, 10). Because DHEA concentrations do not decrease after adrenalectomy and castration, many experiments have been performed with the aim of demonstrating the *de novo* synthesis of DHEA within the brain. DHEA biosynthesis has been demonstrated in cultured glial cells and neurons from the neonatal rat brain (11, 12). In the adult brain, however, a concrete demonstration of the synthesis of DHEA, androstenedione (AD), testosterone, or estradiol directly from endogenous cholesterol has yet to be reported. Sex steroids such as estradiol and testosterone, therefore, have not classically been considered to be "brain-derived neurosteroids." Furthermore, the localization and activity of cytochrome P45017α (CYP17) in adult mammalian brain has also not been demonstrated, despite many sophisticated studies employing immunohistochemistry, molecular biology, and enzyme activity assays (13–16). P45017α has, therefore, been regarded to be only transiently expressed in the brain at embryonic and neonatal stages (11, 12, 14). Recently, a few studies have reported the presence of cytochrome P450 aromatase (P450arom, CYP19) in the adult rat and human hippocampal formation (17, 18).

The present study was designed to examine, in the adult male hippocampus, the cellular localization of P45017α and P450arom and the endogenous metabolism of neurosteroids from PREG. Analyses revealed the neuronal localization of these P450s and the synthesis of DHEA, testosterone, and 17β-estradiol, which suggests their intracrine/paracrine actions on the plasticity of neurons in adult rat brain.

Materials and Methods

Animals. Adult male Wistar rats (3 months old, 210–250 g) were purchased from SLC Japan and Harlan Sprague–Dawley. All experiments using animals in this study were conducted according to the institutional guidelines.

Immunohistochemical Staining of Hippocampal Slices. Immunohistochemical staining was performed essentially as described in refs. 7 and 8. The hippocampi were frozen-sliced with a cryostat. After application of either anti-P45017α IgG (19), at 1/1,000 dilution or anti-P450arom IgG (20) at 1/1,000, the slices were incubated for 18–36 h. Biotinylated anti-rabbit IgG and streptavidin–horseradish peroxidase complex (Vector Laboratories) was applied. Immunoreactive cells were detected in diaminobenzidine-nickel. Fluorescence immunohistochemistry was performed by using streptavidin–Oregon Green 488. For detailed description of the procedures, see *Supporting Text*, which is published as supporting information on the PNAS web site.

Postembedding ImmunoGold Method for Electron Microscopy. Hippocampal slices were prepared by using a vibratome. Freeze substitution and low-temperature embedding of the specimens was performed as described (21). Slices were plunged into liquid propane and immersed in uranyl acetate solution. After polymerization of Lowicryl HM20 resin, ultrathin sections (80 nm

This paper was submitted directly (Track II) to the PNAS office

Abbreviations: PREG, pregnenolone; DHEA, dehydroepiandrosterone; AD, androstenedione; P450arom, cytochrome P450 aromatase; 17β-HSD, 17β-hydroxysteroid dehydrogenase; DHT, dihydrotestosterone.

**To whom correspondence should be addressed. E-mail: kawato@phys.c.u-tokyo.ac.jp

thickness) were cut by using an ultramicrotome. For immunolabeling, sections were incubated with primary antibody against P45017α (1:1,000) or P450arom (1:500) overnight and incubated with secondary gold-tagged (10 nm) Fab fragment in Tris-buffered saline. Sections were counterstained with 1% uranyl acetate and viewed on an electron microscope. For detailed description of the procedures, see *Supporting Text*.

Western Immunoblot Analysis. Microsomes were prepared as described in *Supporting Text* (8). After gel electrophoresis and the transfer to poly(vinylidene fluoride) membranes (Immobilon-P; Millipore), the blots were probed with antibodies against P45017α and P450arom at 1/5,000 dilution and incubated with biotinylated goat anti-rabbit IgG. The membranes were incubated with streptavidin–horseradish peroxidase complex. The protein bands were detected with ECL plus Western blotting detection reagents (Amersham Pharmacia).

RT-PCR and Southern Hybridization. The purified RNAs from rat tissues were reverse-transcribed by using a T-primed first-strand kit (Amersham Pharmacia) (22). Specific primer pairs and the PCR protocols are described in *Supporting Text*. For semiquantitative analysis (see ref. 23), the RT-PCR products were separated on 1.5% agarose gels, stained with ethidium bromide, and analyzed with a fluorescence gel scanner (Atto) and NIH IMAGE software, in comparison with standard curves obtained from PCR of diluted reverse transcribed products (between 1/100 and 1/10,000 in dilution), from testis, ovary, or liver. The PCR products were cloned into TA-cloning vector (Promega) and sequenced. The resulting sequence was identical to the reported cDNA sequences. These cloned products were used as DNA probes for Southern hybridization. After transfer of the RT-PCR products to nylon membrane, Southern hybridization was performed with ^{32}P-labeled cDNA probes for P45017α, P450arom, and GAPDH. Signals were measured by using a BAS-1000 Image analyzer (Fuji film).

HPLC Analysis. Procedures were essentially the same as described in ref. 8. Briefly, the hippocampal cubic slices were incubated with 5×10^6 cpm of [^{3}H]steroids at 28°C in a 1.2 mM Mg^{2+} physiological saline (pH 7.2, consisting of 5 mM Hepes, etc.), into which 95% O_2 gas was bubbled. [^{3}H]steroids (DHEA, estradiol, etc.) were purchased from New England Nuclear, and their specific activities were 22.5–105 Ci/mmol (1 Ci = 37 GBq). After termination of the reaction, the slices were homogenized. To extract steroid metabolites, ethyl acetate/hexane (3:2) was applied to the homogenates. The organic phase was collected by centrifugation, dried, dissolved in an elution solvent of HPLC, and filtrated. The metabolites were separated by using an HPLC system (Jasco, Tokyo). For detailed description of the procedures, see *Supporting Text*.

RIA Analysis. Procedures were essentially the same as described in ref. 8. Briefly, plasma was prepared from trunk blood collected from decapitated rats. The hippocampal cubic slices were incubated at 37°C in 0.1 mM Mg^{2+} physiological saline into which O_2 gas was bubbled. Extraction of steroids were performed as described in HPLC analysis. The estradiol or DHEA fractions were separated by using HPLC with solvent A, and reconstituted in a 0.1 M sodium phosphate buffer containing 0.1% gelatin. The concentration of steroids was measured by means of RIA, which was a competitive reaction assay, for example, between purified estradiol and exogenously added [^{3}H]estradiol against estradiol IgG. Anti-steroid IgG was from ICN. For a detailed description of the procedures, see *Supporting Text*.

Results

Localization and Presence of Cytochrome P450s. Light microscopic investigations of the immunohistochemical staining were performed to determine the cell-specific localization of P45017α and P450arom in the hippocampal formation of adult male rats. Intense

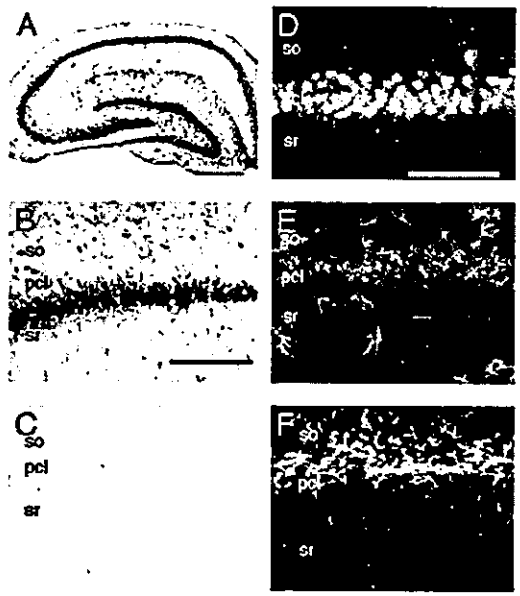

Fig. 1. Immunohistochemical staining of P45017α in the hippocampal formation of an adult male rat. (*A*) The coronal section of the whole hippocampal formation. (*B*) The CA1 region. (*C*) The CA1 stained with anti-P45017α IgG preadsorbed with purified P45017α. (*D*) Fluorescence dual staining of P45017α (green) and neuronal nuclear antigen (red). (*E*) Fluorescence dual staining of P45017α (green) and glial fibrillary acidic protein (red). (*F*) Fluorescence dual staining of P45017α (green) and myelin basic protein (red). In *D–F*, superimposed regions of green and red fluorescence are represented by yellow. so, stratum oriens; pcl, pyramidal cell layer; sr, stratum radiatum. (Scale bar, 800 μm for *A* and 120 μm for *B–F*.)

immunoreactions with anti-P45017α IgG (Fig. 1) and anti-P450arom IgG (Fig. 2) were restricted to pyramidal neurons in the CA1–CA3 regions and to granule cells in the dentate gyrus. The staining shows P45017α and P450arom to be distributed over the entire cell body, in general, and also along the dendrites of the pyramidal neurons in the CA3 region. Neurons were stained with IgG against neuronal nuclear antigen (NeuN). The colocalization of neurons with P45017α and P450arom was demonstrated by using fluorescence dual labeling procedures. Although the NeuN and P450 stainings were nearly superimposed, this was due to the

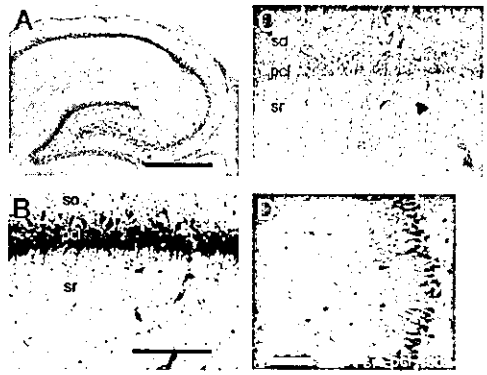

Fig. 2. Immunohistochemical staining of P450arom in the hippocampal formation of an adult male rat. (*A*) The coronal section of the whole hippocampal formation. (*B*) The CA1 region. (*C*) The CA1 stained with P450arom IgG preadsorbed with purified P450arom. (*D*) The CA3, where not only cell bodies but also processes of neurons are densely stained. so, stratum oriens; pcl, pyramidal cell layer; sr, stratum radiatum. (Scale bar, 800 μm for *A* and 120 μm for *B–D*.)

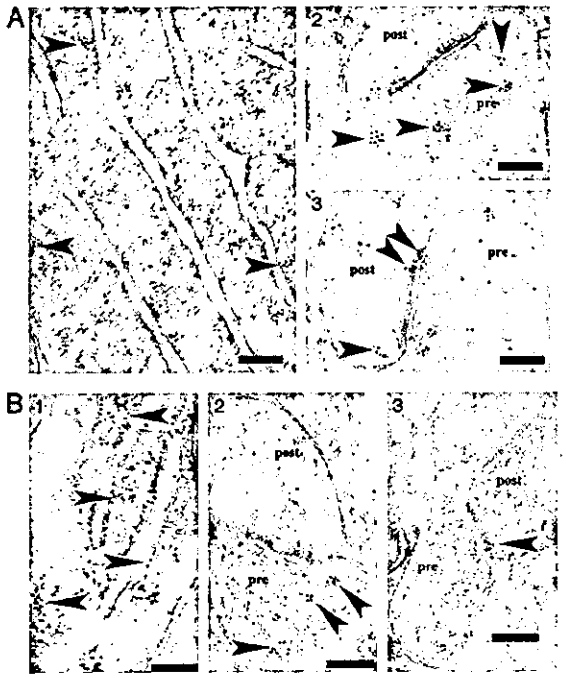

Fig. 3. Immunoelectron microscopic analysis of the distribution of P45017α (*A1–A3*) and P450arom (*B1–B3*) within axospinous synapses, in the strata radiatum of the hippocampal CA1 region at the central region of the rostrocaudal level. Gold particles (indicated with arrowheads) were observed to be localized in the endoplasmic reticulum (*A1* and *B1*), the presynaptic region (*A2* and *B2*), and the postsynaptic region (*A3* and *B3*) of pyramidal neurons. In the axon terminal (*A2* and *B2*), gold particles were associated with small synaptic vesicles (*A2* and *B2*). In dendritic spines, gold particles were found within the head of the spine (*A3* and *B3*). Pre, presynaptic region; Post, postsynaptic region. (Scale bar, 200 nm.)

localization of these cytochromes in the endoplasmic reticulum, distributed over the entire cell bodies, and thus did not indicate a nuclear localization of the cytochromes. Preadsorption of the antibody with an excess of purified guinea pig P45017α or human P450arom antigen (30 μg/ml) resulted in a complete disappearance of the immunoreactivity of these P450s, in all of the positively stained cells in the hippocampus.

The distribution of glial cells was investigated by the immunostaining of marker proteins. Antibodies against glial fibrillary acidic protein (GFAP) of astrocytes, stained star-shaped cells in the strata radiatum, and oriens in the hippocampus. IgG against myelin basic protein (MBP) of oligodendrocytes stained many long fibril cells in the hippocampus. Most of the cells stained with GFAP and MBP IgG were lacking in immunoreactivity to IgG against P45017α and P450arom. This indicates that most of the P45017α- and P450arom-containing cells are neither astrocytes nor oligodendrocytes.

The neuronal localization of P450 was further clarified by ultrastructural investigations. An immunoelectron microscopic analysis using postembedding immunogold was performed to determine the subcellular localization of P45017α and P450arom in hippocampal neurons of adult male rats. P45017α (Fig. 3*A*) and P450arom (Fig. 3*B*) were localized not only in the endoplasmic reticulum but also in both the axon terminals and dendritic spines of principal neurons. Gold particles were clustered in the endoplasmic reticulum of neurons. Gold particles were also localized within the presynaptic compartments, as well as within the postsynaptic compartments. In the presynaptic terminals, gold particles were primarily associated with synaptic vesicles. In dendrites, gold particles were distributed within the cytoplasm of the head of the spine. In some cases, gold particles were affiliated within the postsynaptic density. Preadsorption of the antibody with an excess of P45017α or P450arom antigen (30 μg/ml) resulted in a complete disappearance of the immunoreactivity of these P450s, in all of the positively stained cells.

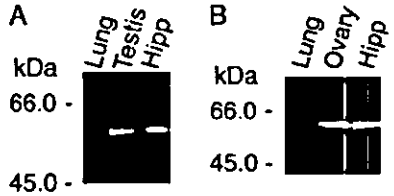

Fig. 4. Western immunoblot analysis of P45017α (*A*) and P450arom (*B*) in microsomes from adult rat. (*A*) Lung (50 μg protein), testis (1 μg), and hippocampus (50 μg). (*B*) Lung (50 μg protein), ovary (1 μg), and hippocampus (50 μg). Lung was used as a negative control.

There were essentially no significant differences between P45017α and P450arom concerning their topographical distribution in neurons. Investigations were performed mainly in the stratum radiatum of the CA1; however, the intraneuronal distribution of gold particles was essentially identical in the CA1, CA3, and dentate gyrus.

The presence of P45017α and P450arom proteins was verified by Western immunoblot analysis. In hippocampal microsomes, single protein bands were observed for P45017α and P450arom (Fig. 4). The concentration of P45017α and P450arom was ≈1/100th to 1/200th of that typical of the testis (P45017α) and ovary (P450arom). The electrophoretic mobility of the P45017α and P450arom bands indicated a molecular mass of ≈57 kDa and 58 kDa, respectively. These molecular masses were approximately equal to those in testis and ovary. Protein bands disappeared when either antibodies were preadsorbed with purified P450 antigens (30 μg/ml).

The level of mRNA transcripts for P45017α and P450arom was investigated by using RT-PCR analyses. The relative number of P450 transcripts expressed in the hippocampus (Fig. 5, lane 5) from adult male rats was demonstrated to be ≈1/200th to 1/300th of those expressed in the testis and ovary, for P45017α and P450arom, respectively. The mRNA levels for P45017α and P450arom in the hypothalamus (Fig. 5, lane 6) were slightly greater (by ≈1.5-fold) than those obtained in the hippocampus. On the other hand, the level of P45017α mRNA in the cerebral cortex (Fig. 5, lane 4) and cerebellum (Fig. 5, lane 7), was $<10^{-4}$ and 10^{-3}, respectively relative to levels observed in the testis. The level of P450arom mRNA, relative to levels in the ovary, was ≈1/500 in the cerebral cortex (Fig. 5, lane 4) and cerebellum (Fig. 5, lane 7).

The expression level of mRNA transcripts for 17β-hydroxy-

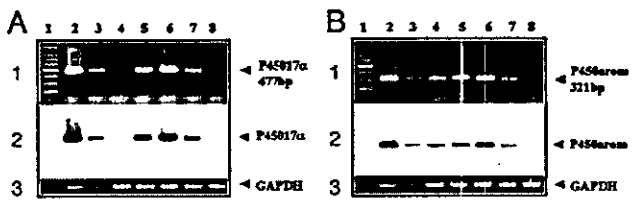

Fig. 5. RT-PCR analysis of mRNAs for P45017α (*A*) and P450arom (*B*) in the adult rat. The RT-PCR products (50 ng each) were visualized with ethidium bromide in *Top*. (*A*) Lane 1, marker (100 bp ladder); lane 2, testis diluted at 1/100; lane 3, testis diluted at 1/1,000; lane 4, cerebral cortex; lane 5, hippocampus; lane 6, hypothalamus; lane 7, cerebellum; lane 8, peripheral blood leukocytes. (*B*) Lane 1, marker; lane 2, ovary diluted at 1/100; lane 3, ovary diluted at 1/1,000; lane 4, cerebral cortex; lane 5, hippocampus; lane 6, hypothalamus; lane 7, cerebellum; lane 8, liver. Peripheral blood leukocytes and liver were used as the negative controls. (*Middle*) Southern hybridizations. (*Bottom*) Ethidium bromide staining of GAPDH

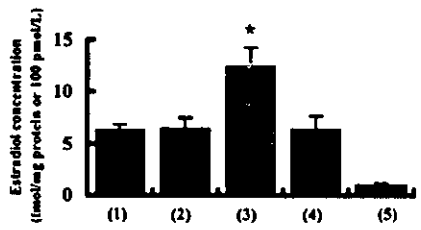

Fig. 6. RIA analysis of estradiol concentrations in adult male rats. Estradiol concentration in the hippocampus before incubation (basal) (column 1), the hippocampus after a 30-min incubation without NMDA (column 2), the hippocampus after a 30-min incubation with 100 μM NMDA (column 3), the hippocampus after a 30-min incubation with 100 μM NMDA in the presence of MK-801 (column 4), and plasma (column 5). The vertical axis indicates the estradiol concentration in fmol/mg protein for the hippocampus (columns 1–4) and in fmol/μl for plasma (column 5). The significance of the NMDA-induced production of estradiol was confirmed by using the Student *t* test (*, $P < 0.05$). The data represent an average over three independent experiments.

steroid dehydrogenase (17β-HSD) (types 1–4) was also investigated by using RT-PCR (data not shown). The level of 17β-HSD mRNA observed in the hippocampus was ≈1/10th relative to the level in the ovary for 17β-HSD (type 1), 1/200th to 1/300th relative to the level in the testis for 17β-HSD (type 3), roughly the same relative to the level in the liver for 17β-HSD (type 4), and $< 10^{-3}$ for 17β-HSD (type 2) relative to the level in the liver.

Steroid Metabolism Assay. The synthesis of estradiol in hippocampal slices was examined by means of a specific RIA using estradiol antibody (ICN) (Fig. 6). The basal concentration of estradiol observed in the hippocampus was 0.60 ± 0.05 fmol/mg wet weight (6.3 ± 0.5 fmol/mg protein; mean ± SEM from three independent experiments). The estradiol basal concentration in the plasma was 0.008 ± 0.039 fmol/μl (≈1.02 fmol/mg protein or 0.098 fmol/mg wet weight), a value considerably lower than that observed in the hippocampus. The *N*-methyl-D-aspartate (NMDA)-inducible production of estradiol was measured by stimulating hippocampal slices with 100 μM NMDA (Biomol) for 30 min. at 37°C in a 0.1 mM Mg^{2+} medium. This treatment increased the concentration of estradiol to 1.35 ± 0.18 fmol/mg wet weight (13.0 ± 1.7 fmol/mg protein), which is nearly twice the estradiol level in hippocampal slices incubated for 30 min without NMDA. Stimulation of net estradiol production with NMDA was completely suppressed by the application of 50 μM MK-801 (a specific blocker of NMDA receptors, Sigma). This enhancement in estradiol synthesis may be due to an increase in the NMDA receptor-mediated Ca^{2+} influx that drives the transport of cholesterol to the inner membrane of mitochondria, followed by a cascade of steroidogenesis (7). The basal concentration of DHEA was also measured in the hippocampus and plasma. The concentration of DHEA was 0.28 ± 0.07 fmol/mg wet weight (2.7 ± 0.7 fmol/mg protein) in the hippocampus, and 0.075 ± 0.036 fmol/μl in plasma. These values are in reasonable agreement with previous publications using DHEA extracts from the whole brain (6).

To analyze the pathway of steroidogenesis, the metabolism of radioactive steroids in hippocampal slices was investigated by using HPLC. To observe the conversion of PREG to DHEA, hippocampal cubic slices from adult male rats were incubated for 0, 1, 3, and 5 h at 28°C, using 5 × 10^6 cpm of [7-^{3}H]PREG as a precursor. Careful attention was given to the removal of all fats from the hippocampal slices during the purification of steroids, before the application to HPLC. A portion of the purified radioactive metabolites (total of 10^6 cpm) was analyzed with an HPLC system, which used an elution liquid composed of hexane/isopropanol/acetic acid (97:3:1) (solvent A). The principal radioactive peak in the tritiated metabolite exhibited a retention time of ≈9.5 min, which was the same as that of [^{14}C]DHEA used as a standard (Fig. 7*A*). A time-dependent increase in the [^{3}H]DHEA fractions was observed over a period of 5 h (Fig. 8*A*, which is published as supporting

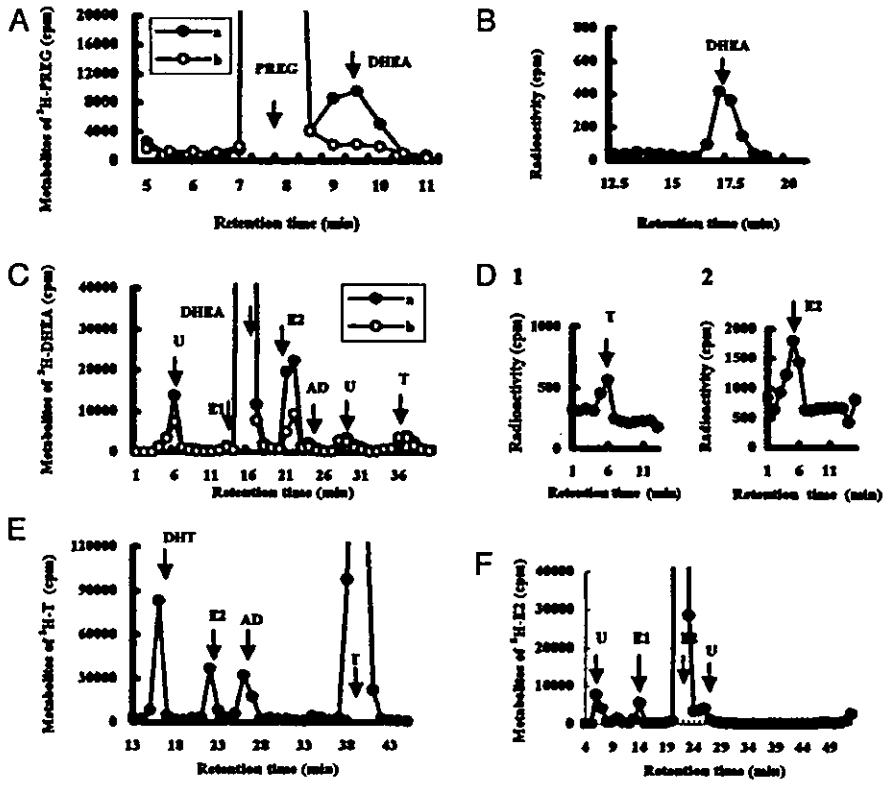

Fig. 7. HPLC analysis of steroid metabolism in adult rat hippocampal slices. A total of 10^6 cpm purified metabolites were applied to HPLC. (*A*) HPLC profiles of [^{3}H]PREG metabolites using elution solvent A. Slices were incubated for 5 h in the absence (line a) or in the presence (line b) of SU-10603. (*B*) Reverse-phase HPLC (solvent C) of [^{3}H]DHEA fractions from line a in *A*. (*C*) Profiles of [^{3}H]DHEA metabolites (solvent B) in the absence (line a) or in the presence (line b) of fadrozole, after incubation of slices for 5 h. (*D*) Reverse-phase HPLC (solvent C) of [^{3}H]testosterone (*D1*) and [^{3}H]estradiol (*D2*) taken from peaks T and E2, respectively, in *C*. (*E*) Profiles (solvent B) of [^{3}H]testosterone metabolites after incubation of slices for 5 h. (*F*) Profiles (solvent B) of [^{3}H]estradiol metabolites after a 5-h incubation. The arrows designate the elution peak position of the standard [^{14}C]steroid with abbreviations: E1 (estrone), T (testosterone), and E2 (estradiol). "U" designates unknown metabolites. The vertical axis indicates ^{3}H radioactivity (cpm). The retention time of the (same) standard [^{14}C]steroid differed slightly among *C*, *E*, and *F* due to the different silica gel columns used. More than three independent experiments were performed for each of these analyses.

information on the PNAS web site). Analysis of the steroid extract (adjusted to a total of 10^6 cpm) indicated that the amount of [^{3}H]DHEA (product), relative to [^{3}H]PREG (substrate), increased from $0.0 \times 10^4/1.0 \times 10^6$ (0 h) to $1.0 \times 10^4/0.98 \times 10^6$ (1 h), $2.9 \times 10^4/0.97 \times 10^6$ (3 h), and $4.6 \times 10^4/0.96 \times 10^6$ (5 h). Note that trilostane (Mochida) was included in these experiments to facilitate observation of the net production of [^{3}H]DHEA by inhibiting 3β-hydroxysteroid dehydrogenase (3β-HSD). Trilostane prevents the conversion of DHEA to AD and of PREG to progesterone. The application of a specific inhibitor of P45017α, SU-10603 (Novartis) at 10 μM, reduced the production of [^{3}H]DHEA to ≈21% of the control value. To exclude the possibility of contamination from other radioactive metabolites, the three fractions having a retention time of 9–10 min were combined and subjected to a second round of HPLC analysis. The column was eluted with a different elution solvent B (hexane/isopropanol/acetic acid = 98:2:1) for the normal phase HPLC (Fig. 8*B*), and with solvent C (acetonitrile/H_2O = 40:60) for the reverse-phase HPLC (Fig. 7*B*), to improve the resolution. A single radioactive peak of [^{3}H]metabolite having the same retention time as that of [^{14}C]DHEA was observed in this second round of HPLC. These results indicate the significant enzymatic activity of P45017α in the hippocampus, which is responsible for the conversion of PREG to DHEA.

To investigate the conversion of DHEA to testosterone and estradiol, hippocampal slices were incubated with 5×10^6 cpm of [1,2,6,7-^{3}H]DHEA for 5 h at 28°C, and the purified metabolites (total of 10^6 cpm) were analyzed by using HPLC. When elution solvent B was used, several eluent peaks were observed (Fig. 7*C*). The eluent peak with a retention time of 37 min was designated as testosterone by comparison with the standard [^{14}C]testosterone. The eluent peak exhibiting a retention time of 21–22 min was close to the position of [^{14}C]estradiol. To improve the resolution, these fractions were collected and subjected to a second round of HPLC analysis using solvent D (hexane/isopropanol/acetic acid = 99:1:1). A single peak, with a retention time of 51 min, was observed, which is in good agreement with [^{14}C]estradiol (Fig. 8*C*). An additional round of analysis, using reverse-phase HPLC and solvent C, was performed for the HPLC fractions corresponding to estradiol, testosterone, and AD. These metabolites were again observed to elute at the same positions obtained for the standard [^{14}C]steroids (Fig. 7*D*). Analysis of the steroid extract (10^6 cpm) indicated that the relative amount of [^{3}H]estradiol (product) to [^{3}H]DHEA (substrate) increased from $0.0 \times 10^4/1.0 \times 10^6$ (0 h) to $3.5 \times 10^4/0.90 \times 10^6$ (1 h), $5.5 \times 10^4/0.88 \times 10^6$ (3 h) and $6.4 \times 10^4/0.86 \times 10^6$ (5 h).

To confirm the participation of P450arom in estradiol synthesis, fadrozole (Novartis) was used to inhibit the activity of P450arom. A 30-min preincubation with 100 μM fadrozole, applied before the addition of [^{3}H]DHEA, suppressed the conversion of [^{3}H]DHEA to estradiol considerably (to ≈34% of the control), but had no suppressive effect on its conversion to testosterone (to ≈102% of the control) (Fig. 7*C*). The conversion from testosterone to estradiol and dihydrotestosterone (DHT) was then investigated. Hippocampal slices were incubated with [1,2,6,7-^{3}H]testosterone (5×10^6 cpm) for 0, 1, 2, 3, 4, and 5 h at 28°C, and the purified metabolites (total of 10^6 cpm) were analyzed with HPLC using solvent B (Fig. 7*E*). A time-dependent increase in [^{3}H]estradiol, [^{3}H]DHT, and [^{3}H]AD was observed (Fig. 8*D*). Analysis of the steroid extracts (10^6 cpm) indicted that the relative amount of [^{3}H]estradiol (product) to [^{3}H]testosterone (substrate) increased from $0.0 \times 10^4/1.0 \times 10^6$ (0 h) to $0.7 \times 10^4/0.90 \times 10^6$ (1 h), $1.9 \times 10^4/0.87 \times 10^6$ (3 h) and $3.8 \times 10^4/0.84 \times 10^6$ (5 h). The absence of other contaminating metabolites in these estradiol fractions was confirmed by means of a second round of HPLC using solvent C (for normal phase HPLC) and D (for reverse-phase HPLC).

HPLC analysis of AD and estrone metabolites are described in *Supporting Text*. Finally, the conversion of estradiol to other metabolites was also investigated by incubating [2,4,6,7-^{3}H]estradiol (5×10^6 cpm) with hippocampal slices for 5 h. Only very small amounts of metabolites such as estrone and testosterone were observed (Fig. 7*F*), suggesting that estradiol was not significantly inactivated but may remain stable.

Discussion

Our results not only demonstrated the distribution of P45017α and P450arom in pyramidal and granule neurons at the light microscopic level (Figs. 1 and 2), but also indicated that these P450 proteins were specifically localized in pre- and post-synaptic locations and the endoplasmic reticulum of these neurons by electron microscopy, with a single molecule (gold particle) resolution (Fig. 3). These findings, combined with the results of steroid metabolism assays, strongly suggest that estradiol is endogenously synthesized in neurons from cholesterol in the hippocampal formation. These results indicate the need to reconsider the belief that these sex steroids are produced only in the gonads and reach the target brain via blood circulation. Rather, such steroids may be produced endogenously in the adult brain, where they play an essential role in the plasticity and protection of neurons.

Pathway of Steroidogenesis in the Hippocampus. In our previous work, the steroid synthesis was triggered by exposing neurons to NMDA, which induced a Ca^{2+} influx through the NMDA receptors and resulted in the significant production of PREG(s) (5, 7). A pool of full-length (37-kDa) steroidogenic acute regulatory protein (StAR) was processed to the truncated 30-kDa StAR upon NMDA stimulation (7). The expression of essential steroidogenic proteins [StAR, P450scc (CYP11A1), and 3β-HSD] in the hippocampal principal neurons was demonstrated by means of immunostaining and Western blot analysis (7–9) or by *in situ* hybridization (17, 22). The presence of mRNAs for 17β-HSD types 1–4 has been demonstrated in the human hippocampus (24). In the rat hippocampus, 17β-HSD (type 1) has been shown to be localized in neurons by immunostaining (25). Previous studies have shown the immunoreactivity of 5α-reductase in the rat hippocampus (16, 26).

In combination with these results, the current observations suggest that hippocampal neurons are equipped with a set of enzymes to catalyze the synthesis of estradiol from cholesterol. Neurosteroid synthesis may therefore proceed in the following manner. First, cholesterol is transported with StAR into the inner membrane of mitochondria, and converted to PREG by P450scc. After reaching the microsomes, P45017α converts PREG to DHEA. Then DHEA to AD by 3β-HSD, 17β-HSD (type 3) catalyzes the conversion of AD to testosterone. This is followed by a further transformation to estradiol by P450arom. It appears that estradiol is also formed by 17β-HSD (type 1) from estrone, which is converted from AD by P450arom.

The rate of production of steroid metabolites was rather low. The amount of [^{3}H]DHEA formed from [^{3}H]PREG, that of [^{3}H]estradiol from [^{3}H]DHEA, and that of [^{3}H]estradiol from [^{3}H]testosterone each represented ≈4.6–6.4% of the total radioactivity obtained by using [^{3}H]steroid precursors, observed after 5-h incubation (Fig. 7). Several reasons are considered for this. First, the binding of exogenously applied [^{3}H]steroid to P450s in hippocampal slices is likely to be very inefficient, as such steroids must penetrate deeply into cells in the thick slices to reach enzymes, without being absorbed by nonspecific binding to hydrophobic membranes, and replace endogenous steroid substrates already bound to the enzymes. Second, the conversion rate from [^{3}H]PREG to [^{3}H]DHEA by P45017α may indeed be extremely low; as a result, no previous study could detect this low activity. Third, not only [^{3}H]DHEA but also other steroids such as sulfated DHEA and 7-hydroxyDHEA (27) may be produced in parallel from [^{3}H]PREG. Fourth, [^{3}H]estradiol is not a unique metabolite from [^{3}H]testosterone, but DHT and other steroids may also be produced in parallel. These multiple pathways, including backward reactions, may be a primary reason of the observed low efficiency of steroid metabolism, because of the

presence of sulfotransferase, 5α-reductase, and cytochrome P4507b (16, 26, 28). These factors could reduce the rate of production for [^{3}H]DHEA and [^{3}H]estradiol to 4.6–6.4% of the total radioactivity.

To verify that the observed low levels of radioactive metabolites were real products, we performed a set of control experiments. We observed a considerable decrease in [^{3}H]DHEA production by the presence of SU-10603, inhibitor of P45017α (Fig. 7*A*). In addition, estradiol production was suppressed considerably by the presence of fadrozole, an inhibitor of P450arom (Fig. 7*C*). These results indicate that the observed steroid metabolite levels are above the detection limit of the HPLC analysis. The background radioactivity in the HPLC profiles in Fig. 7 was <300 cpm at any position, using hippocampal slices fixed with paraformaldehyde to inactivate steroidogenic enzymes before incubation with ^{3}H-substrate steroids.

Glial cells have been considered to play an important role in neurosteroidogenesis, as many reports have indicated the presence of mRNA and steroidogenic activity for P450scc, P45017α, 3β-HSD, and 17β-HSD in cultures of astrocytes and oligodendrocytes (6, 11, 12, 29, 30). Based on these studies, the following steroidogenic sequence is suggested in the neonatal rat brain. The primary source of PREG is the oligodendrocytes. PREG is then transferred to the astrocytes, where it is converted to DHEA, and further metabolized to sex steroids (11, 12). It should be noted, however, that these studies, which use primary glial cell cultures, can be performed only for embryonic and neonatal brain. As a result, direct information is not available from these studies regarding the biosynthesis of neurosteroids in adult rat brain. The possibility of glial steroidogenesis in the adult hippocampal formation cannot be excluded by the present study, as a weak staining of P450scc (7), P45017α, and P450arom was observed in some glia-like cells.

Previous Understanding of P45017α and P450arom in the Brain. A direct demonstration of the neuronal synthesis of DHEA in adult mammalian brain has not previously been reported, although the presence of significant amounts of DHEA had been noted (15, 10). It has therefore been assumed that DHEA and the sex steroids are supplied to the brain via the blood circulation (6, 15, 20). As reported in a number of studies, the absence of P45017α and its activity in the brain of adult mammals has discouraged the investigation of the endogenous synthesis of sex steroids and DHEA in adult brain (13–16). Incubations of [^{3}H]PREG with brain slices and microsomes from rat and mouse, had failed to produce [^{3}H]DHEA (15). Moreover, many attempts to demonstrate the immunohistochemical reactivity for P45017α in the rat brain had been unsuccessful (13). mRNAs for P45017α had not been detected in adult rat brain by either RNase protection assays or RT-PCR (14). The expression of the mRNA for P45017α had been reported by many laboratories as only transient, occurring during rat embryonic and neonatal development (11, 12, 31). Although a similar level of P45017α mRNA had been reported in both astrocytes and neurons in primary cultures from the brain of neonatal rats, neurons had exhibited a much lower metabolic activity than astrocytes for the conversion of PREG to DHEA (11, 12). Such investigations, which use primary cell cultures, are not possible for adult brains, because cells from adult brains cannot be cell cultured.

Our observation of a significant amount of P45017α mRNA was achieved due to (*i*) a careful design of primers to not include sequences that may form stable loops, inhibiting binding to mRNA, (*ii*) the use of isolated rat hippocampal formation, rather than brain mixtures where the cortex did not express P45017α mRNA, and (*iii*) the considerable improvement in the last few years of the commercially available enzymes such as *Taq* polymerase used for RT-PCR.

The role of P450arom in the hippocampus had also not been well elucidated, primarily because many studies had indicated the absence of P450arom in the adult rat and mouse hippocampus (20, 32). Recently, however, the significant expression of mRNA for P450arom in the pyramidal and granule neurons of the adult rat hippocampus has been demonstrated by using *in situ* hybridization (17). The level of the mRNA expression in the adult mouse hippocampus was approximately half of that in neonatal stages (23). The activity of P450arom has been suggested in the adult male rat hippocampus based on the results of the testosterone-induced protection of the hippocampal neuronal death induced by the domoic acid-treatments (3).

Modulation by Estradiol of Hippocampal Neurons. Investigations have been focused on female rats regarding the chronic, delayed effects of estradiol on synaptic plasticity. For example, the dendritic spine density in pyramidal neurons is sensitive to the estrous cycle (1, 33) and also to experimentally induced estrogen depletion and replacement, which serve to modulate estrogen levels in blood circulation (4). Estradiol also induces rapid effects. A 20-min preperfusion of 1–10 nM estradiol induced the rapid modulation of long-term potentiation of the CA1 neurons in the hippocampal slices (2). Our elucidation of the estradiol-synthesis in principal neurons, which begins with cholesterol, introduces an essentially a new supply of brain neurosteroids, in addition to gonads. Estradiol synthesis may be dependent on NMDA receptor-mediated Ca^{2+} influx, thereby dependent on synaptic communication (5, 7). The concentration of endogenously synthesized estradiol by NMDA stimulation (≈0.75 nM; see Fig. 6, column 3) should be sufficient to modulate these neuronal activities, because the local concentration of estradiol (at the site of synthesis) may transiently be an order of magnitude higher than the mean concentration of 0.75 nM.

We thank Dr. J. Rose for critical reading of the manuscript. We thank Novartis for the kind gift of SU-10603. This work was supported in part by National Institutes of Health Grant PO1AG16765 (to J.H.M.).

1 Woolley, C. S., Weiland, N. G., McEwen, B. S. & Schwartzkroin, P. A. (1997) *J. Neurosci.* **17**, 1848–1859.
2 Foy, M. R., Xu, J., Xie, X., Brinton, R. D., Thompson, R. F. & Berger, T. W. (1999) *J. Neurophysiol.* **81**, 925–929.
3 Azcoitia, I., Sierra, A., Veiga, S., Honda, S., Harada, N. & Garcia-Segura, L. M. (2001) *J. Neurobiol.* **47**, 318–329.
4 Pozzo-Miller, L. D., Inoue, T. & Murphy, D. D. (1999) *J. Neurophysiol.* **81**, 1404–1411.
5 Shibuya, K., Takata, N., Hojo, Y., Furukawa, A., Yasumatsu, N., Kimoto, T., Enami, T., Suzuki, K., Tanabe, N., Ishii, H. *et al.* (2002) *Biochim. Biophys. Acta* **25462**, 1–16.
6 Baulieu, E. E. (1997) *Recent Prog. Horm. Res.* **52**, 1–32.
7 Kimoto, T., Tsurugizawa, T., Ohta, Y., Makino, J., Tamura, H., Hojo, Y., Takata, N. & Kawato, S. (2001) *Endocrinology* **142**, 3578–3589.
8 Kawato, S., Hojo, Y. & Kimoto, T. (2002) *Methods Enzymol.* **357**, 241–249.
9 Kawato, S., Yamada, M. & Kimoto, T. (2003) *Adv. Biophys.* **37**, 1–48.
10 Corpechot, C., Robel, P., Axelson, M., Sjovall, J. & Baulieu, E. E. (1981) *Proc. Natl. Acad. Sci. USA* **78**, 4704–4707.
11 Zwain, I. H. & Yen, S. S. C. (1999) *Endocrinology* **140**, 880–887.
12 Zwain, I. H. & Yen, S. S. C. (1999) *Endocrinology* **140**, 3843–3852.
13 Le Goascogne, C., Sananes, N., Gouezou, M., Takemori, S., Kominami, S., Baulieu, E. E. & Robel, P. (1991) *J. Reprod. Fertil.* **93**, 609–622.
14 Mellon, S. H. & Deschepper, C. F. (1993) *Brain Res.* **629**, 283–292.
15 Baulieu, E. E. & Robel, P. (1998) *Proc. Natl. Acad. Sci. USA* **95**, 4089–4091.
16 Mensah-Nyagan, A. G., Do-Rego, J. L., Beaujean, D., Luu-The, V., Pelletier, G. & Vaudry, H. (1999) *Pharm. Rev.* **51**, 63–81.
17 Wehrenberg, U., Prange-Kiel, J. & Rune, G. M. (2001) *J. Neurochem.* **76**, 1879–1886.
18 Stoffel-Wagner, B., Watzka, M., Schramm, J., Bidlingmaier, F. & Klingmuller, D. (1999) *J. Steroid Biochem. Mol. Biol.* **70**, 237–241.
19 Shinzawa, K., Ishibashi, S., Murakoshi, M., Watanabe, K., Kominami, S., Kawahara, A. & Takemori, S. (1988) *J. Endocrinol.* **119**, 191–200.
20 Lakab, R. I., Horvath, T. L., Leranth, C., Harada, N. & Naftolin, F. (1992) *J. Steroid Biochem. Mol. Biol.* **44**, 481–498.
21 Adams, M. M., Shah, R. A., Janssen, W. G. M. & Morrison, J. H. (2001) *Proc. Natl. Acad. Sci. USA* **98**, 8071–8076.
22 Furukawa, A., Miyatake, A., Ohmichi, T. & Ichikawa, Y. (1998) *J. Neurochem.* **71**, 2231–2238.
23 Ivanova, T. & Beyer, C. (2000) *Cell Tissue Res.* **300**, 231–237.
24 Beyenburg, S., Watzka, M., Blumcke, I., Schramm, J., Bidlingmaier, F., Elger, C. E. & Stoffel-Wagner, B. (2000) *Epilepsy Res.* **41**, 83–91.
25 Pelletier, G., Luu-The, V. & Labrie, F. (1995) *Brain Res.* **704**, 233–239.
26 Melcangi, R. C., Celotti, F., Castano, P. & Martini, L. (1993) *Endocrinology* **132**, 1252–1259.
27 Jellinck, P., Lee, S. J. & McEwen, B. S. (2001) *Steroid Biochem. Mol. Biol.* **78**, 313–317.
28 Rose, K., Stapleton, G., Dott, K., Kiely, M. P., Best, R., Schwarz, M., Russel, D. W., Bjorkhem, I., Seckl, J. & Lathe, R. (1997) *Proc. Natl. Acad. Sci. USA* **94**, 4925–4930.
29 Jung-Testas, I., Hu, Z. Y., Baulieu, E. E. & Robel, P. (1989) *Endocrinology* **125**, 2083–2091.
30 Papadopoulos, V. (1993) *Endocr. Res.* **14**, 222–240.
31 Compagnone, N. A., Bulfone, A., Rubenstein, J. L. R. & Mellon, S. H. (1995) *Endocrinology* **136**, 5212–5223.
32 Lauber, M. T. & Lichtensteiger, W. (1994) *Endocrinology* **135**, 1611–1068.
33 Woolley, C. S. & McEwen, B. S. (1994) *J. Neurosci.* **14**, 7680–7687.

ELSEVIER

Biochimica et Biophysica Acta 1619 (2003) 301–316

BIOCHIMICA ET BIOPHYSICA ACTA
BBA

www.bba-direct.com

Review

Hippocampal cytochrome P450s synthesize brain neurosteroids which are paracrine neuromodulators of synaptic signal transduction

Keisuke Shibuya[a], Norio Takata[a], Yasushi Hojo[a,b], Aizo Furukawa[b,c], Nobuaki Yasumatsu[a], Tetsuya Kimoto[a,b], Taihei Enami[a], Kumiko Suzuki[a], Nobuaki Tanabe[a], Hirotaka Ishii[a], Hideo Mukai[a,b], Taiki Takahashi[a,b], Taka-aki Hattori[a,b], Suguru Kawato[a,b,*]

[a] *Department of Biophysics and Life Sciences, Graduate School of Arts and Sciences, University of Tokyo at Komaba, Meguro, Tokyo 153, Japan*
[b] *CREST, Japan Promotion of Science and Technology, University of Tokyo at Komaba, Meguro, Tokyo 153, Japan*
[c] *Department of Biochemistry, Faculty of Medicine, Kagawa Medical University, Kagawa 761, Japan*

Received 5 February 2002; received in revised form 24 September 2002; accepted 30 September 2002

Abstract

Hippocampal pyramidal neurons and granule neurons of adult male rats are equipped with a complete machinery for the synthesis of pregnenolone, dehydroepiandrosterone, 17β-estradiol and testosterone as well as their sulfate esters. These brain neurosteroids are synthesized by cytochrome P450s (P450scc, P45017α and P450arom) from endogenous cholesterol. Synthesis is acutely dependent on the Ca^{2+} influx attendant upon neuron–neuron communication via *N*-methyl-D-aspartate (NMDA) receptors. Pregnenolone sulfate, estradiol and corticosterone rapidly modulate neuronal signal transduction and the induction of long-term potentiation via NMDA receptors and putative membrane steroid receptors. Brain neurosteroids are therefore promising neuromodulators that may either activate or inactivate neuron–neuron communication, thereby mediating learning and memory in the hippocampus.

Keywords: neurosteroid; P450; hippocampus; brain; LTP; signal transduction

1. Introduction

The aim of this article is to describe brain P450 research that has been focused on the mammalian hippocampus, an attractive new field in neuroscience. Although the purification of steroids from brain tissues, which are very fatty, has been extremely difficult, a number of previous studies have successfully demonstrated the presence and accumulation of several neurosteroids, including pregnenolone (PREG), dehydroepiandrosterone (DHEA) and their sulfate esters (PREGS and DHEAS) in the mammalian brain [1,2]. In each case, the reported concentration of the brain steroid was an order of magnitude greater than that typical of plasma. Adrenolectomy did not decrease the level of PREG(S) and DHEA(S) in the brain, suggesting the de novo synthesis of these steroids within the brain [1,3]. Active neurosteroidogenesis has, however, not been well elucidated, due to the extremely low levels of steroidogenic proteins in the brain [4]. Sex steroids (e.g., 17β-estradiol and testosterone) have not been considered to be brain neurosteroids, because of the reported absence of cytochrome P45017α in adult mammalian brain [5,6]. In particular, because sex steroids cannot be synthesized without P45017α, which converts PREG to DHEA (a precursor steroid), they are thought to reach the brain via blood circulation [7]. To date, because a good correlation between

Abbreviations: AMPA, α-amino-3-hydroxy-5-methyl-4-isoxazole propionic acid; CORT, corticosterone; cytochrome P450scc (CYP11A1), cytochrome P450 having cholesterol side-chain cleavage activity; cytochrome P45017α (CYP17A), cytochrome P450 catalyzing the conversion of pregnenolone to dehydroepiandrosterone; cytochrome P450arom (CYP19), cytochrome P450 catalyzing aromatization of androstenedione and testosterone; DHEA, dehydroepiandrosterone; GABA, γ-aminobutyric acid; GAPDH, glyceraldehyde-3-phosphate dehydrogenase; 3β-HSD, 3β-hydroxysteroid dehydrogenase; 17β-HSD, 17β-hydroxysteroid dehydrogenase; NMDA, *N*-methyl-D-aspartate; PREG, pregnenolone; PREGS, pregnenolone sulfate; RIA, radioimmunoassay; StAR, steroidogenic acute regulatory protein

* Corresponding author. Department of Biophysics and Life Sciences, Graduate School of Arts and Sciences, University of Tokyo at Komaba, Meguro, Tokyo 153, Japan. Tel./fax: +81-3-5454-6517.
E-mail address: kawato@phys.c.u-tokyo.ac.jp (S. Kawato).

0304-4165/02/$ - see front matter
PII: S0304-4165(02)00489-0

progesterone synthesis and its nerve regeneration had mainly been shown for peripheral Schwann cells [8,9], the term 'neurosteroids' has been used to refer to neuroactive steroids produced not only in the brain, but also in the peripheral nerves and glial cells.

The hippocampus, which is involved essentially in learning and memory processes, is known to be a target for the neuromodulatory actions of the steroid hormones produced in the adrenal glands and gonads. In addition to hormones derived from the endocrine glands, hippocampal neurons are exposed to locally synthesized brain neurosteroids. In contrast to the classical genomic effects of peripheral steroids, many neurosteroids induce non-genomic effects by means of putative cell surface receptors [10–12]. There is increasing evidence that neurosteroids modulate neurotransmissions rapidly (<30 min) and with either excitatory or inhibitory effects, in the hippocampus, the center for learning and memory [2,13]. PREGS potentiates the Ca^{2+} conductivity of the *N*-methyl-D-aspartate (NMDA) subtype of glutamate receptors [14,15] but suppresses the Cl^- conductivity of the γ-aminobutyric acid (GABA) receptors in cultured rat hippocampal neurons [16,17]. Taken in combination, these actions could facilitate the excitation of neurons at the postsynaptic level [16]. DHEA potentiates the GABA-induced Cl^- current but DHEA sulfate suppresses it [16–18]. Several studies have reported the observation of specific, non-genomic effects induced by estradiol on neuronal excitability in the hippocampus, which indicates the non-reproductive actions of sex steroids [13,19–21].

Neurosteroids are indicated to be effective in enhancing animal learning and memory. The administration of PREGS and DHEA enhanced the retention of foot-shock avoidance in mice when injected directly into the hippocampus [22,23]. An injection of PREGS into the hippocampus has also been reported to temporally improve the spatial memory performance of aged rats [24–26].

Until recently, the cellular location and activity of the neurosteroidogenic machinery in the brain had not been sufficiently elucidated. This is due primarily to the very low level of expression of the mRNAs of steroidogenic enzymes in the cerebrum and cerebellum [4]. For example, the concentration of P450scc mRNA expressed in the brain is reported to be only 10^{-4}–10^{-5} of that in the adrenal gland [6,27]. As a result, the presence of P450scc mRNA could be demonstrated only by the reverse transcription–

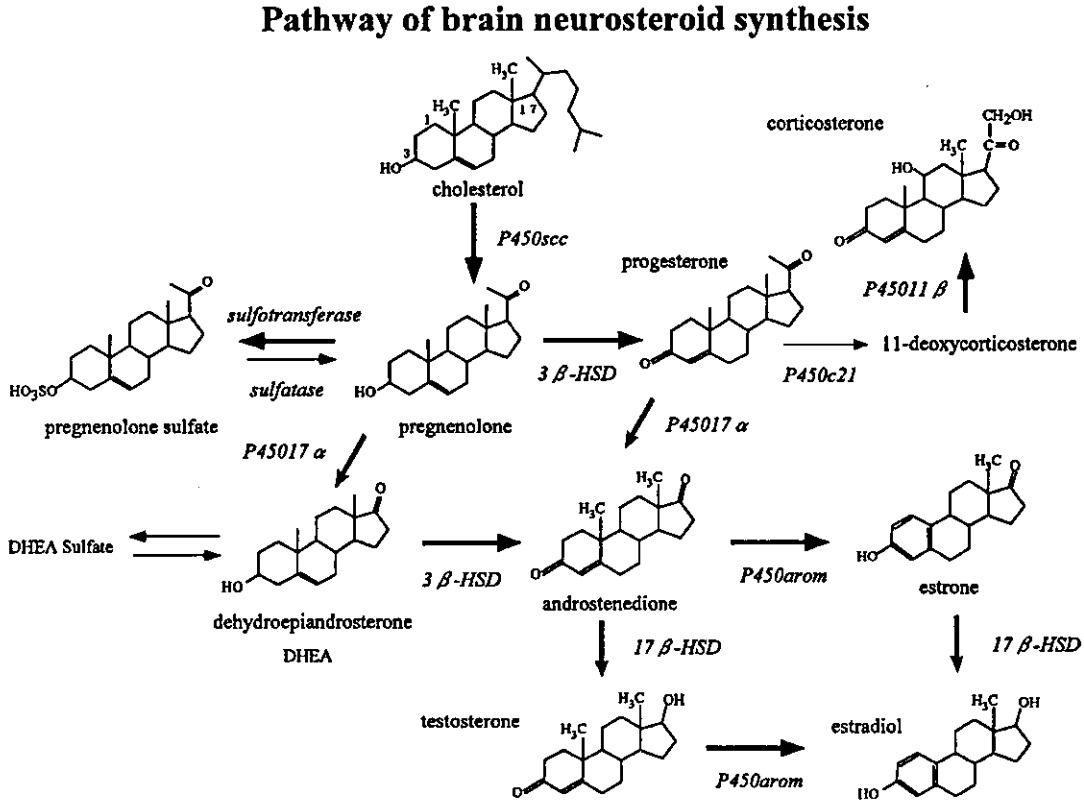

Fig. 1. Flow chart of brain neurosteroid synthesis in hippocampal neurons. The structures of brain neurosteroids and enzymes responsible for biotransformation are indicated. Thick arrows indicate pathways demonstrated in the hippocampus. Thin arrows indicate possible pathways expected to be present in the hippocampus.

polymerase chain reaction (RT-PCR) method. The role of neurons in steroid synthesis had not yet been clearly determined, although glial cells had been subjected to extensive investigation [28,29]. The localization, in neurons of several steroidogenic proteins, has been demonstrated by means of in situ hybridization. For example, mRNAs for both steroidogenic acute regulatory protein (StAR) and 3β-hydroxysteroid dehydrogenase (3β-HSD) mRNA (10^{-2}–10^{-3} of the levels in the adrenal gland) were observed to be localized along the pyramidal cell layer in the CA1–CA3 regions and the granule cell layer in the dentate gyrus [30]. Expression of mRNAs for steroidogenic factor-1 in colocalization with StAR and P450arom has been demonstrated in rat and marmoset hippocampus [31]. There had been still poor demonstration of the neuron-specific localization of steroidogenic P450s in the hippocampus, although the neuronal localization of P450scc and 3β-HSD had been demonstrated in Purkinje neurons in the rat cerebellum [32].

In this work, the localization of the neurosteroidogenic machinery in hippocampal neurons is described, along with the associated synthesis of a variety of brain neurosteroids (including sex steroids). The rapid, non-genomic effects of neurosteroids on synaptic transmission are also described. Let the term, 'brain neurosteroid' refer to a steroid that is synthesized de novo in the brain by P450 systems. This includes all of the steroids illustrated in Fig. 1.

2. Localization of neurosteroidogenic systems in the adult rat hippocampus

2.1. Immunohistochemical and Western immunoblot analysis

Adult male Wistar rats aged 3 months were used, and the hippocampi were frozen-sliced coronally at 20 μm thickness with a cryostat. A significant localization of cytochromes P450scc, P45017α and P450arom was observed in pyramidal neurons in the CA1–CA3 regions, as well as in granule cells in the dentate gyrus, by means of the immunohistochemical staining of hippocampal slices [28,29,33,34]. The colocalization of P450s with hydroxysteroid sulfotransferase and StAR has also been demonstrated in pyramidal neurons and granule cells [29].

To determine the localization of P450scc, an immunohistochemical staining was performed with anti-rat P450scc antibodies against amino acid sequence 421–441 (Fig. 2) [29]. The resulting intense immunoreaction with P450scc IgG was restricted to pyramidal neurons in the CA1–CA3 regions, and to granule cells in the dentate gyrus. The colocalization of immunoreactivity against P450scc and NeuN confirmed the presence of P450scc in these neurons. Immunohistochemical staining was also performed to determine the presence of other cytochrome P450s, such as P45017α and P450arom, using anti-guinea pig P45017α IgG (gift from Dr. Shiro Kominami) and anti-human P450arom IgG (gift from Dr. N. Harada). The observation of an intense immunoreaction with all of these antibodies was limited to pyramidal neurons in the CA1–CA3 regions and granule cells in the dentate gyrus (Fig. 3) [28]. The 3β-HSD activity was also observed to be localized in these neurons, the activity of which was stained by means of formazan accumulation. Both hydroxysteroid sulfotransferase and StAR were also stained with antibodies against rat hydroxysteroid sulfotransferase (gift from Dr. Hiro-omi Tamura) and mouse StAR (gift from Dr. Douglas Stocco) [29]. These results, taken together, imply that pyramidal neurons and granule cells are equipped with complete steroidogenic systems which catalyze the conversion of cholesterol to PREG, DHEA, testosterone and estradiol, and their subsequent sulfation to PREGS and DHEAS.

The expression of these steroidogenic proteins was confirmed by Western immunoblot analysis. As illustrated in Fig. 4, a single protein band was observed for each of these P450s [34]. The resulting molecular weights obtained for P450scc, P45017α and P450arom were almost identical to those obtained from peripheral steroidogenic organs. The relative levels of these P450s in the hippocampus were approximately 1/500 (P450scc) and 1/200 (P45017α and P450arom) of that in the testis (P450scc and P45017α) and the ovary (P450arom), respectively.

In marked contrast to the peripheral steroidogenic organs, only the full-length 37-kDa species of StAR was observed in the mitochondria from the control hippocampus (Fig. 5) [29]. The level of StAR in the hippocampus was approximately 1/100 of that in rat testis. When the hippocampus was stimulated with 100 μM NMDA for 30 min, conversion of StAR from the 37-kDa species to the truncated 30-kDa species was observed. The processing of StAR proteins, which is probably performed by mitochondrial proteases, was dependent on an NMDA-mediated-Ca^{2+} influx. This processing of StAR may be correlated with the Ca^{2+}-dependent movement of StAR-bearing cholesterol from the outer to the inner membranes of mitochondria, which supplies cholesterol to P450scc. This possibility was further investigated using genetically engineered Chinese hamster ovary (CHO) cells. Upon heat-shock treatment at 43 °C for 2 h, this stable transfectant CHO line expressed NMDA receptors which were mouse GluRε1(NR2A) with GluRξ1(NR1) subunits [35]. When these CHO cells were transfected with StAR plasmid for 48 h, a large proportion of full-length, 37 kDa StAR (approximately 45%) was observed by a Western blot analysis of the mitochondrial fractions. Upon application of 100 μM NMDA for 10 min, a sustained Ca^{2+} elevation induced the conversion of approximately 95% of the full-length StAR to the truncated 30-kDa species (K. Shibuya, H. Ishii, H. Mukai and S. Kawato, unpublished results).

For decades, neurosteroidogenesis had been extensively studied in glial cells. This line of investigations was

motivated by the absorption of anti-bovine P450scc antibodies by white matter throughout the rat brain [36,37], and by the many reports which have indicated the presence of steroidogenic proteins and mRNAs in astrocytes, oligodendrocytes and white matter [36,38,39]. We therefore examined the possible existence of P450s in glial cells. The distributions of astroglial cells and oligodendroglial cells, however, displayed very different patterns from those characteristic of the P450-containing cells (see Fig. 2) [29]. The distributions of astroglial and oligodendroglial

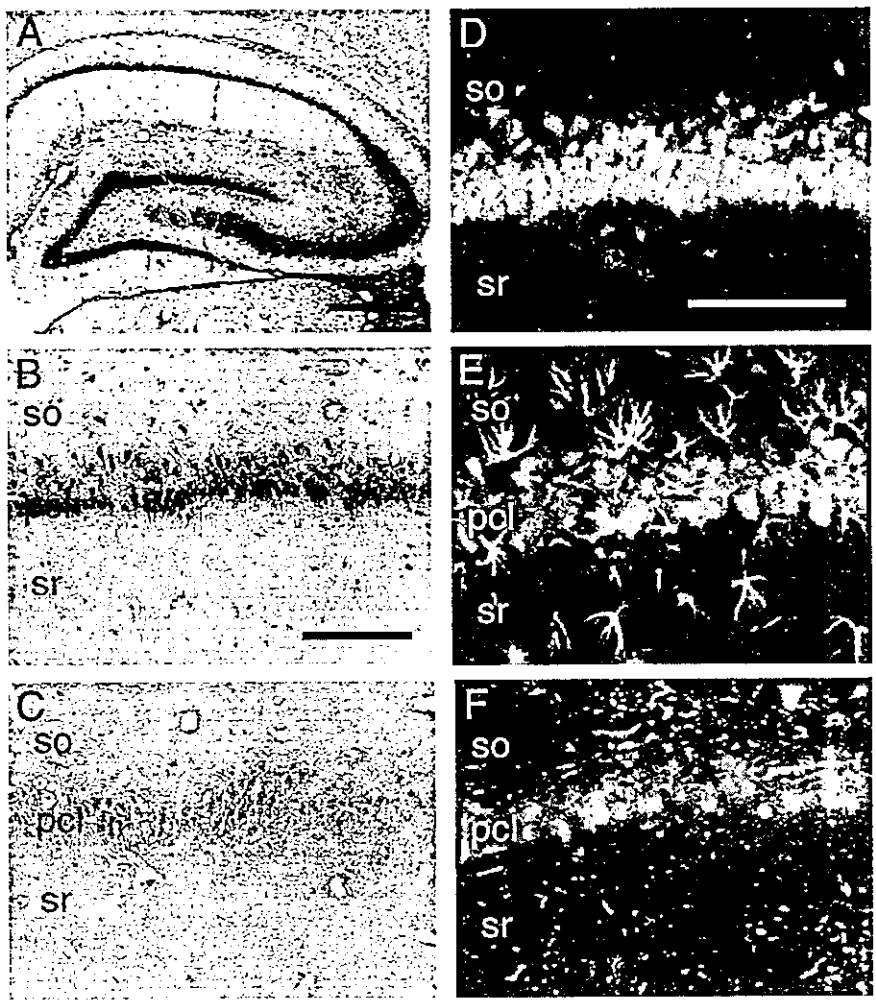

Fig. 2. Immunohistochemical staining of cytochrome P450scc, astroglial cells and oligodendroglial cells in hippocampal slices of an adult male rat. Adult male Wistar rats aged 3 months (from SLC Japan Co.) were deeply anesthetized with pentobarbital and perfused transcardially with phosphate-buffered saline, followed by a fixative solution (4% paraformaldehyde) at 4 °C. The hippocampi were postfixed for 24–48 h in the fixative solution at 4 °C and were frozen-sliced coronally at 20 μm thickness with a cryostat (Leica CM1510, Germany) at −17 °C. All experiments using animals were conducted according to the institutional guidelines. (A) Low-magnification image of the whole hippocampus, stained with antibodies against rat cytochrome P450scc. The somata layer of pyramidal neurons is characterized as a mirror image of C-shaped curve throughout the CA1–CA3 regions of the hippocampus. Granule cells in the dentate gyrus (DG) showed a characteristic arrowhead distribution. (B) The hippocampal CA1 region stained with antibodies against rat P450scc. (C) Preadsorption of the antibody with excess purified bovine P450scc antigen is observed to result in the disappearance of P450scc immunoreactivity in all of the positively stained cells in CA1 region, due to cross-reaction of the anti-rat P450scc antibodies. (D) Fluorescence dual staining of P450scc (green) and NeuN (red). (E) Fluorescence dual staining of P450scc (green) and glial fibrillary acidic protein (GFAP) (red). (F) Fluorescence dual staining of P450scc (green) and myelin basic protein (MBP) (red). A superimposed region of green and red fluorescence is represented in yellow color. (G) Astroglial cells stained with antibody GFAP. (H) Oligodendroglial cells stained with antibody against MBP. B and C, D–F, G and H are at the same magnification. Scale bar, 800 μm (A), 120 μm (B and C, G and H), and 100 μm (D–F). so, stratum oriens; pcl, pyramidal cell layer; sr, stratum radiatum. A–C, G and H are obtained using the avidin–biotin–peroxidase complex (ABC) technique according to the free-floating method, and immunoreactive cells are visualized by diaminobenzidine–nickel staining. Fluorescence immunohistochemistry of P450scc in E and F is carried out in the same manner as ABC staining except that the avidin–horseradish peroxidase complex is replaced by streptavidin–Oregon Green 488 complex. Detection of neuronal/glial marker proteins was achieved with Cy3-labeled anti-mouse IgG without avidin–biotin amplification. Fluorescence signals are observed using a confocal microscope. (A–F are taken from Kimoto et al. [29].)

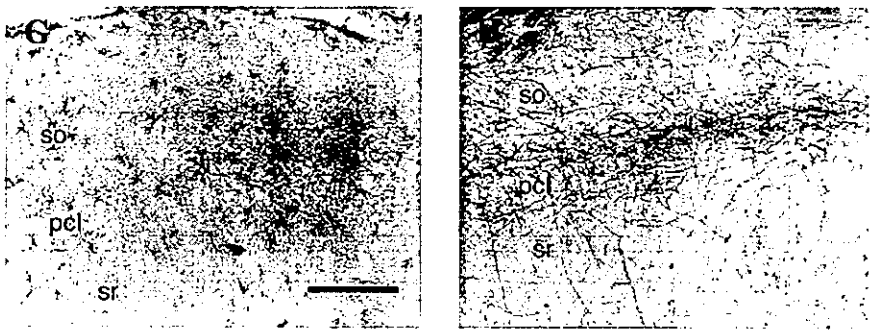

Fig. 2 (*continued*).

cells (each stained with their specific antibodies) are clearly different from those of P450-reactive cells. Glial cells were observed mainly in the stratum radiatum and the stratum oriens (see Fig. 2). This indicates that the majority of P450-containing cells are neither astroglial cells nor oligodendroglial cells.

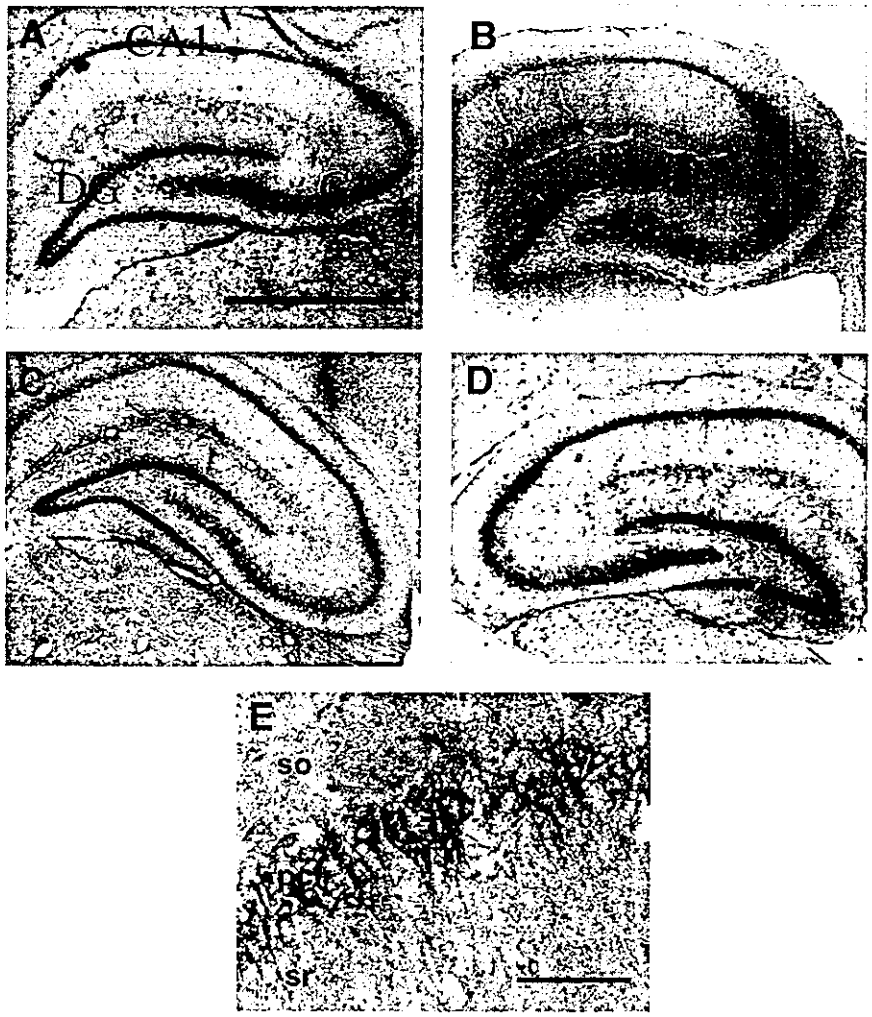

Fig. 3. Immunohistochemical staining of P45017α, P450arom, the sulfotransferase and StAR in the hippocampus of adult male rats. (A) P45017α in the whole transverse section of the hippocampus; (B) P450arom; (C) the sulfotransferase; (D) StAR protein; (E) activity of 3β-HSD in the CA1 region as revealed by nitro-BT staining. Observation of P45017α, P450arom, the sulfotransferase, StAR and 3β-HSD is restricted to pyramidal neurons in the CA1–CA3 regions and granule cells in the dentate gyrus (DG). so, stratum oriens; pcl, pyramidal cell layer; sr, stratum radiatum. (A–D) A low magnification; (E) the high magnification. Scale bar, 800 (A–D) and 120 μm (E). Immunoreactive cells in A–D are visualized with diaminobenzidine–nickel staining. (Taken from Kimoto et al. [29].)

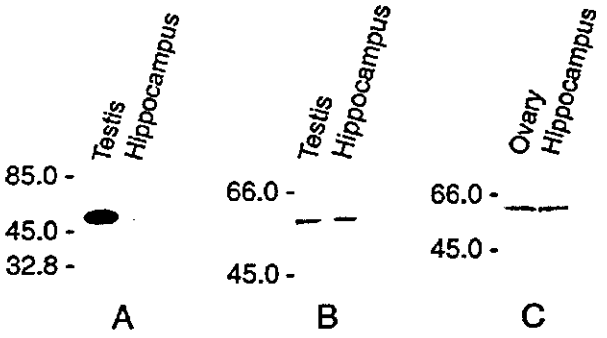

Fig. 4. Western immunoblot analysis of steroidogenic proteins in hippocampal tissues of adult male rats. (A) P450scc in mitochondria; (B) P45017α in microsomes; (C) P450arom in microsomes. For each panel, the left lane indicates a positive control protein band in rat testis (1 μg protein for A and 0.5 μg protein for B) or ovary (0.5 μg protein), and the right lane indicates a protein band in the hippocampus (50 μg protein). Numbers along the vertical direction indicate molecular weights. None of these protein bands are observed in the lung used as a negative control. (Taken from Kawato et al. [28,34].)

2.2. Transcripts for P450s in the hippocampus

The PCR amplification of mRNA transcripts for cytochromes P450scc, P45017α and P450arom was performed using a total RNA Purification Kit (Nippongene, Japan). The hippocampal tissues from adult male rats aged 3 months were used. The relative number of P450 transcripts expressed in the hippocampus was demonstrated to be $1/10^4$–$1/10^5$ for P450scc, approximately 1/300 for both P45017α and P450arom (A. Furukawa and S. Kawato, unpublished results), when compared with those expressed in the adrenal gland (for P450scc), the testis (for P45017α) and the ovary (for P450arom). Not only the PCR amplification but also the ribonuclease (RNase) protection assay demonstrated the presence of StAR transcripts with an expression level of approximately 1/200 of the levels in the adrenal gland. The RNase protection assay for P450scc in the hippocampus, which was performed using a ^{32}P-labelled rat P450scc antisense riboprobe, however, yielded no detectable specific hybridization signals [30]. Collectively, the relative level of mRNA expressed in the hippocampus was lowest for P450scc and highest for StAR, with that of P45017α and P450arom expressed at intermediate levels.

The mRNA levels obtained for P45017α and P450arom in the hypothalamus were almost twice of those obtained in the hippocampus (A. Furukawa, unpublished results). In the

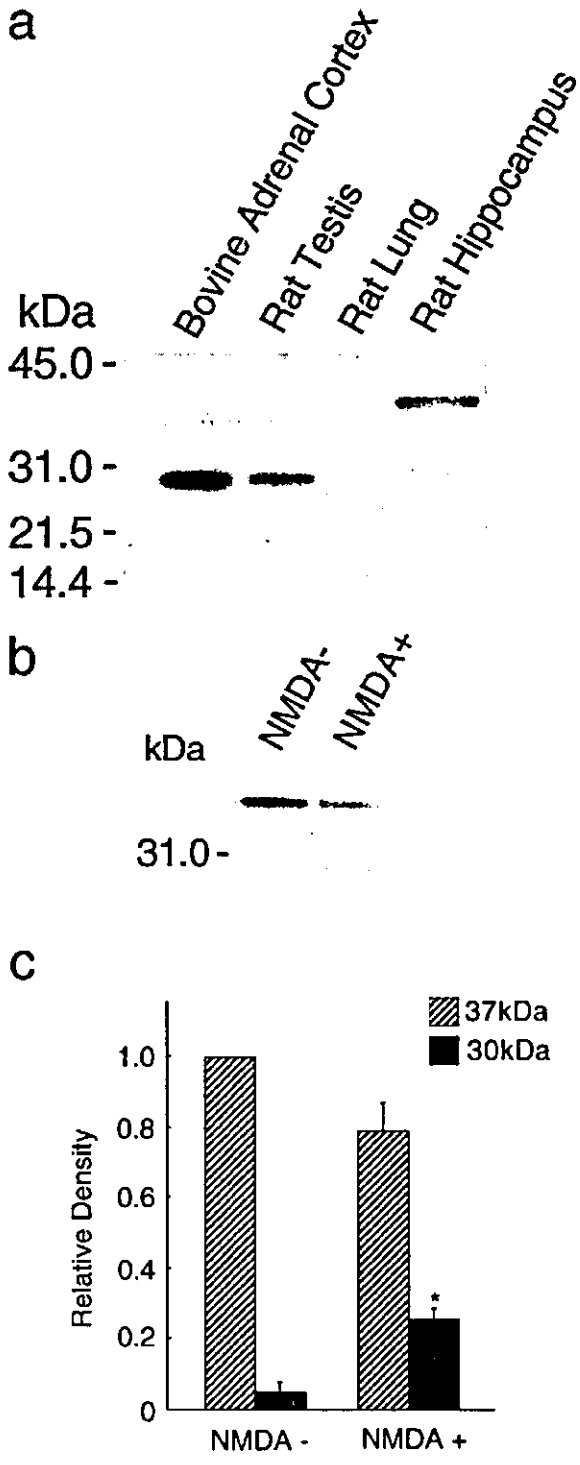

Fig. 5. Western immunoblot analysis of StAR in mitochondria from the hippocampal tissues of adult male rats. (a) From left to right, mitochondria from bovine adrenal cortex (1 μg protein), rat testis (1 μg protein), rat lung (50 μg protein), and rat hippocampus (50 μg protein). Rat lung mitochondria were used as a negative control. Mitochondria from bovine adrenal cortex and rat testis were used as a positive control. (b) Effect of NMDA stimulation on StAR in hippocampal mitochondria. Left lane, mitochondria incubated without NMDA for 30 min; right lane, mitochondria stimulated with 100 μM NMDA for 30 min. Upper and lower bands correspond to 37000 and 30000 in molecular weight, respectively. Each lane contained 50 μg protein. (c) Quantitative comparison for immunoblots of StAR in mitochondria from the hippocampus. Data represent the mean ± S.E. from three independent experiments and are expressed as a relative density compared with that of the 37-kDa StAR bands in the mitochondria obtained without stimulation by NMDA. *$P<0.05$ compared with the density of 30 kDa StAR from the hippocampus incubated without NMDA. (Taken from Kimoto et al. [29].)

cerebral cortex, however, the mRNA expression for P45017α was not detectable within the experimental error, which indicates that the cerebral cortex levels were lower than those in the peripheral steroidogenic organs by at least a factor of 10^{-4}.

3. Neurosteroid synthesis

3.1. Analysis with specific radioimmunoassay (RIA)

The activity of the steroidogenic system in the hippocampus from adult male rats was measured by means of RIA using a RIA kit from ICN (USA) for PREG and 17β-estradiol [29,33.34]. Note that PREGS was analyzed using antibodies against PREG after solvolysis to PREG [29]. The purification of neurosteroids from very fatty brain tissues required the application of a set of sophisticated methods, which included purification with organic solvent, column chromatography and high-performance liquid chromatography (HPLC), etc. [29,40,41]. The basal concentrations of PREG and PREGS which were measured in the hippocampus were 0.17 and 0.29 pmol/mg protein (i.e., 0.016 and 0.028 pmol/wet weight, 16 and 28 nM), respectively, which were roughly eight times greater than those typical of plasma [29]. To demonstrate the acute net production of neurosteroids during neuron–neuron communication, the NMDA-stimulated production of PREG and PREGS was investigated in hippocampal cubic slices [29] (see Fig. 6). Upon stimulation with 100 μM NMDA for 30 min at 37 °C, the hippocampal level of PREG and PREGS increased to 0.35 and 0.60 pmol/mg protein (33 and 57 nM), respectively, which represents an approximate doubling of the basal levels. Stimulation of PREG and PREGS production with NMDA was completely suppressed by either the application of MK-801 (a specific blocker of NMDA receptors), or by the depletion of extracellular Ca^{2+}. This suggests that the NMDA-induced production of PREG was mediated by the influx of Ca^{2+} through NMDA receptors. The application of aminoglutethimide (an inhibitor of P450scc) completely blocked the PREG production induced by NMDA stimulation. This indicates that the PREG production in the hippocampus was due solely to the P450scc enzyme activity. The

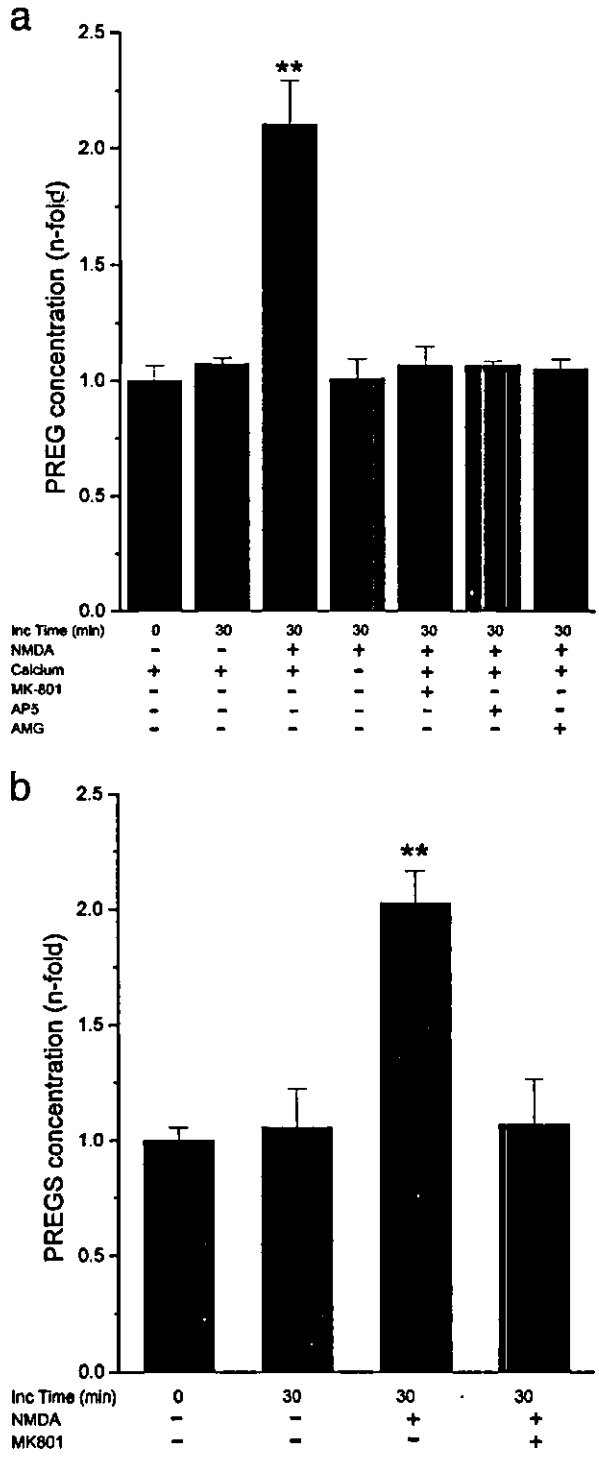

Fig. 6. RIA analysis of the synthesis of PREG and PREGS in hippocampal cubes. (a) PREG concentration. From left to right, basal PREG (without incubation); PREG after incubation in the absence of NMDA and inhibitors; PREG after incubation with 100 μM NMDA; PREG after incubation with 100 μM NMDA in Ca^{2+}-depleted medium; PREG after incubation with 100 μM NMDA in the presence of 50 μM MK-801; PREG after incubation with NMDA in the presence of AP5; and PREG after incubation with NMDA and 1 mM aminoglutethimide. (b) PREGS concentration. From left to right, basal PREGS (without incubation); PREGS after incubation in the absence of NMDA and inhibitors; PREGS after incubation with 100 μM NMDA; PREGS after incubation with NMDA in the presence of MK-801. All incubations were performed for 30 min at 37 °C. Vertical scale in each panel indicates the relative PREG or PREGS concentration normalized by the basal values (0.165 pmol/mg protein for PREG and 0.294 pmol/mg protein for PREGS). Each column represents the mean ± S.E. of four to seven independent determinations, each analyzed in duplicate. $^{**}P < 0.01$ compared with the PREG or PREGS concentration in the case of the 30-min incubation without NMDA stimulation. (Taken from Kimoto et al. [29].)

concentration of 17β-estradiol was also investigated. The basal concentration of estradiol was approximately 0.006 pmol/mg protein (600 pM) which is roughly six times greater than that typical of plasma. When the hippocampal slices were stimulated with 100 μM NMDA for 30 min at 37 °C, the estradiol concentration increased to approximately 0.013 pmol/mg protein (1.3 nM).

3.2. Analysis with HPLC

The synthesis of DHEA and estradiol in the hippocampal cubic slices was also investigated by means of HPLC analysis [28,34]. The elution solvent employed consisted of hexane/isopropanol/acetic acid = 97:3:1 or 98:2:1. The significant conversion of [^{3}H]-PREG (10^6 cpm) to [^{3}H]-DHEA (approximately 7000 cpm) was observed after incubation with the slices for 30 min to 5 h at 20 °C [28]. When [^{3}H]-DHEA (10^6 cpm) was incubated with hippocampal slices for 5 h at 20 °C, the production of significant amounts of [^{3}H]-androstenedione, [^{3}H]-testosterone and [^{3}H]-estradiol (approximately 4000 cpm) was observed. The approximate relative ratio of production was androstenedione/testosterone/estradiol = 1:2:17, which demonstrates the effective synthesis of estradiol. It should be noted that the production of [^{3}H]-estradiol obtained from [^{3}H]-PREG as the initial substrate was much smaller than that obtained from [^{3}H]-DHEA. This is probably due to the additional multiple steroidogenic pathways from PREG, as compared to pathways from DHEA.

4. Rapid action of neurosteroids

4.1. NMDA receptor-mediated Ca^{2+} signals

The NMDA receptor-mediated elevation of the intracellular calcium concentration ($[Ca^{2+}]_i$) was investigated by means of digital fluorescence microscopy (ARGUS-50 system, Hamamatsu Photonics, Japan), using the Ca^{2+}-sensitive indicator, fura-2 or Calcium Green-1 [42,43].

4.1.1. Effect of PREGS

For isolated hippocampal neurons taken from 3-day-old rats and cultured for 8–10 days, the application of 100 μM NMDA induced a transient elevation in $[Ca^{2+}]_i$ which lasted for approximately 20–60 s in 86% of the neurons, in the absence of steroids, and in Mg^{2+}-free medium. Preincubation with 100 μM PREGS for 20 min at 37 °C increased both the peak amplitude of the Ca^{2+} transients by 1.4-fold, and the population of NMDA-responsive neurons from 86% to 92%. Application of PREGS caused no considerable change in the time course of NMDA-induced Ca^{2+} transients [42,43].

The PREGS-induced enhancement of the Ca^{2+} transients was also examined in genetically engineered CHO cells using imaging analysis. Upon heat-shock treatment at 43 °C for 2 h,

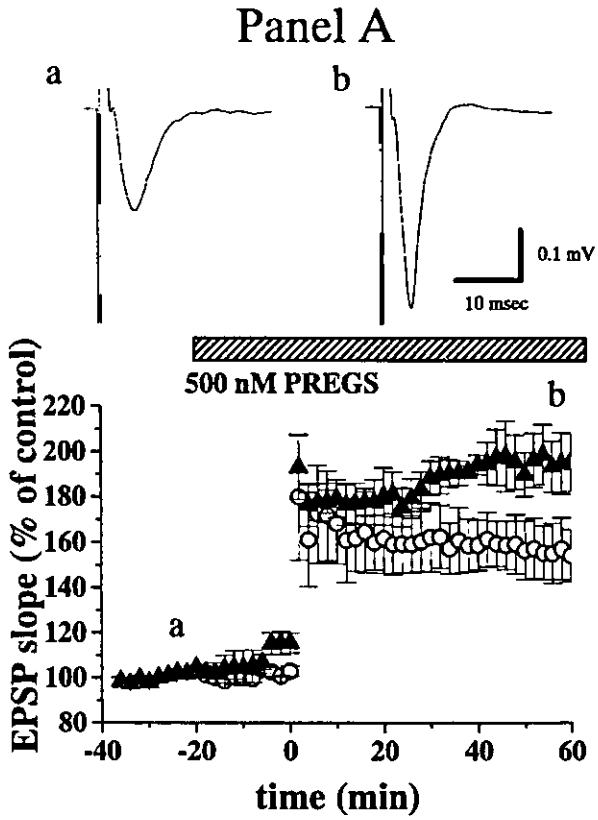

Fig. 7. Electrophysiological measurements of the LTP induction of the field EPSP in the CA1 pyramidal neurons in hippocampal slices from 4-week-old rats. (Panel A) Enhancement of LTP induction by perfusion of PREGS. Upper panel: (a and b) EPSP slopes in the presence of 500 nM PREGS, showing sample recordings taken before (a) and after (b) tetanus stimulation, at times corresponding to similarly lettered points on the graphs. Lower panel: Changes in slopes of the EPSP, plotted against the ordinate scale. Here, 100% refers to the response value before tetanic stimulation, irrespective of the test condition. Tetanic stimulation was delivered at time, $t = 0$. The applied concentrations of PREGS are 0 (drug free, open circle) and 500 nM (closed triangle). Points for each of the two conditions illustrated represent the means of 12 observations. Hatched bar above the graph indicates the period of time during which PREGS was administered. (Panel B) Suppression of LTP induction by perfusion of estradiol. Upper panel: (a and b) EPSP slopes in the presence (a and b) and absence (c and d) of 10 nM estradiol, taken before (a and c) and after (b and d) the tetanus stimulation. Lower panel: Changes in the slope of the EPSP upon the tetanus stimulation at time, $t = 0$. Estradiol concentration is 0 (open circle), 0.1 (closed circle), 1.0 (open triangle), 10 (closed triangle) and 50 nM (open square), respectively. Hatched bar above the graph indicates period of time during which estradiol was administered. (Panel C) Suppression of LTP induction by perfusion with CORT. Upper panel: (a and b) EPSP slopes in the presence (a and b) and absence (c and d) of 10 μM estradiol, taken before (a and c) and after (b and d) the tetanic stimulation. Lower panel: Changes in the slopes of the EPSP upon the tetanic stimulation. CORT concentration is 0 (open circle) and 10 μM (closed triangle). Hatched bar above the graph indicates the period of time during which CORT was administered. [Panel A, unpublished results of N. Takata and S. Kawato. Panels B and C, unpublished results of N. Yasumatsu and S. Kawato.]

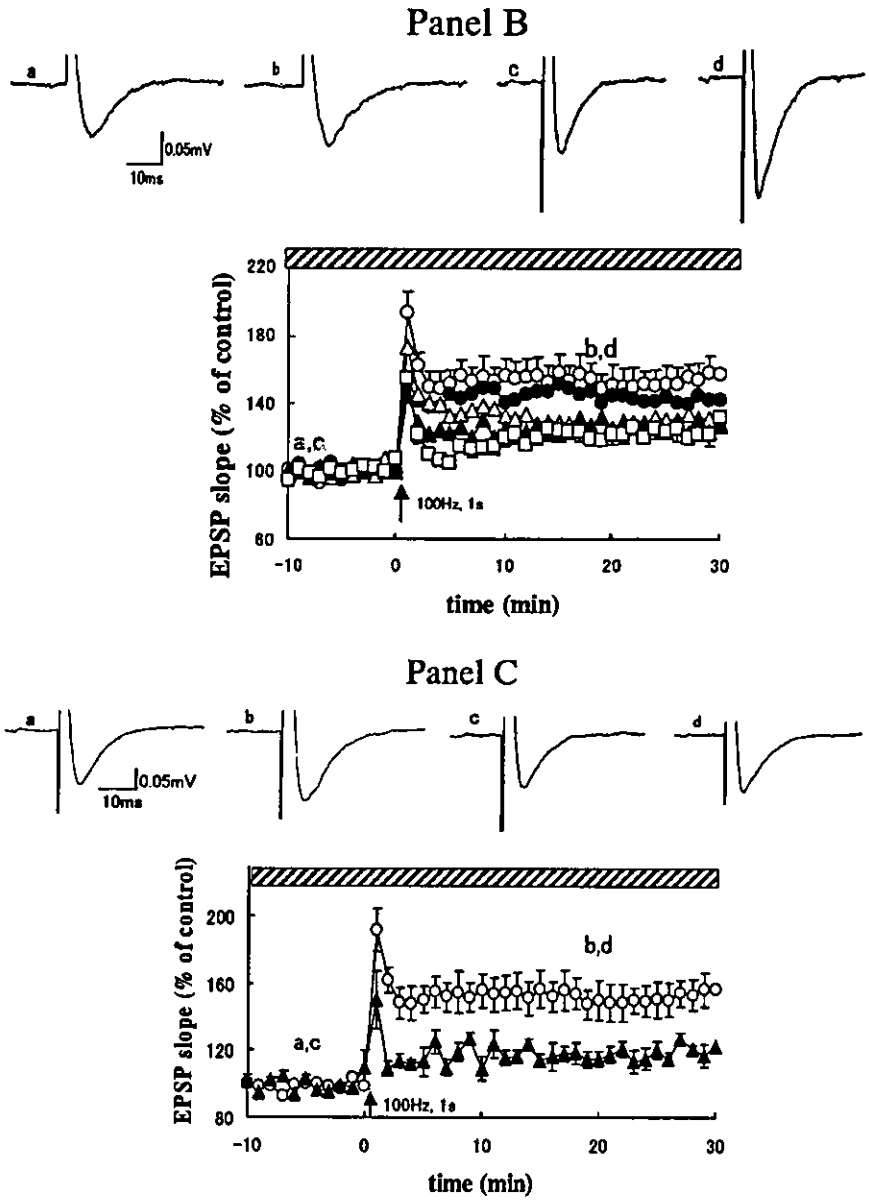

Fig. 7 (*continued*).

this stable transfectant CHO line expressed NMDA receptors which were either mouse GluRε1(NR2A) with GluRζ1(NR1) subunits or GluRε2(NR2B) with GluRζ1(NR1) subunits [35]. In contrast to hippocampal neurons, these CHO cells demonstrated a sustained Ca^{2+} elevation upon NMDA stimulation. The application of 50 μM PREGS for 20 min enhanced the NMDA-induced Ca^{2+} elevation by approximately 2-fold [44]. This PREGS-induced enhancement was canceled by the coapplication of PREGS with other sulfated steroids (e.g., DHEAS and estradiol sulfate), indicating that the sulfate residue is essential for their action on NMDA receptors. Taken in combination with intracellular electrophysiological measurements combined with NMDA stimulation [17,45,46], these results imply that PREGS increases the opening probability of NMDA receptors.

4.1.2. Effect of corticosterone (CORT)

CORT is a principal glucocorticoid that is synthesized in the rodent (e.g., rat and mouse) adrenal cortex and secreted in response to stress [47]. To date, little has been reported concerning the rapid effects (i.e., those which appear within 30 min of application) of CORT on neurotransmitter-mediated signal transduction in hippocampal neurons. We examined the acute effects of CORT using digital fluorescence microscopy, with the Ca^{2+}-sensitive indicator, fura-2 [42,43]. CORT induced a rapid effect on NMDA receptor-